

## Up-regulation of GPR48 Induced by Down-regulation of p27<sup>Kip1</sup> Enhances Carcinoma Cell Invasiveness and Metastasis

Yun Gao,<sup>1</sup> Kyoko Kitagawa,<sup>1</sup> Yoshihiro Hiramatsu,<sup>1,3</sup> Hirotohi Kikuchi,<sup>1,3</sup> Tomoyasu Isobe,<sup>1</sup> Mai Shimada,<sup>1,4</sup> Chiharu Uchida,<sup>1</sup> Takayuki Hattori,<sup>1</sup> Toshiaki Oda,<sup>1</sup> Keiko Nakayama,<sup>5</sup> Keiichi I. Nakayama,<sup>6</sup> Tatsuo Tanaka,<sup>2</sup> Hiroyuki Konno,<sup>3</sup> and Masatoshi Kitagawa<sup>1</sup>

Departments of <sup>1</sup>Biochemistry 1 and <sup>2</sup>Endoscopic and Photodynamic Medicine, <sup>3</sup>Second Department of Surgery, and <sup>4</sup>Oral and Maxillofacial Surgery, Hamamatsu University School of Medicine, Hamamatsu, Shizuoka, Japan; <sup>5</sup>Division of Developmental Genetics, Center for Translational and Advanced Animal Research on Human Diseases, Tohoku University Graduate School of Medicine, Sendai, Miyagi, Japan; and <sup>6</sup>Department of Molecular and Cellular Biology, Medical Institute of Bioregulation, Kyushu University, Higashi-ku, Fukuoka, Japan

### Abstract

A reduced expression level of the cyclin-dependent kinase inhibitor p27<sup>Kip1</sup> is associated with increased tumor malignancy and poor prognosis in individuals with various types of cancer. To investigate the basis for this relation, we applied microarray analysis to screen for genes differentially expressed between p27<sup>+/-</sup> and parental (p27<sup>+/+</sup>) HCT116 human colon carcinoma cells. Expression of the gene for G protein-coupled receptor 48 (GPR48) was increased in the p27<sup>+/-</sup> cells. Forced expression of GPR48 increased both *in vitro* invasive activity and lung metastasis potency of HCT116 cells. In contrast, depletion of endogenous GPR48 by RNA interference reduced the invasive potential of HeLa and Lewis lung carcinoma cells not only *in vitro* but also *in vivo*. Moreover, GPR48 expression was significantly associated with lymph node metastasis and inversely correlated with p27 expression in human colon carcinomas. GPR48 may thus play an important role in invasiveness and metastasis of carcinoma and might therefore represent a potential prognostic marker or therapeutic target. (Cancer Res 2006; 66(24): 11623-31).

### Introduction

Metastasis is a major clinical determinant of the poor prognosis of various human cancers. There are enormous studies indicating biological markers associated with distant metastasis, including lymph node metastasis. The expression of a cyclin-dependent kinase (CDK) inhibitor p27<sup>Kip1</sup> (hereafter p27) is reduced in many types of human cancer, including breast (1, 2) and colorectal (3) carcinomas, and it is inversely related to tumor aggressiveness and directly associated with prognosis in individuals with such cancers (4). p27 functions as an important negative regulator of the cell cycle by inhibiting the activity of G<sub>1</sub> cyclin-CDK complexes during G<sub>0</sub> and G<sub>1</sub> phases (5). Degradation of p27 results in the activation of G<sub>1</sub> cyclin-CDK complexes and consequent promotion of cell cycle progression from G<sub>1</sub> to S phase. Elimination of p27 is regulated by

SCF<sup>Skp2</sup>, an SCF-type ubiquitin ligase that catalyzes the ubiquitylation of p27 and thereby targets it for degradation by the 26S proteasome (6). Kip1 ubiquitylation-promoting complex was also recently identified as a ubiquitin ligase for p27 that promotes G<sub>1</sub> progression (7). The reduced abundance of p27 in human tumors results from enhanced degradation of this protein by the ubiquitin-proteasome pathway (8, 9). Expression of Skp2 is increased in certain transformed cell lines and various types of human cancer (10). Such increased expression of Skp2 may enhance the degradation of p27 and thereby promote cell cycle progression. However, accelerated cell growth alone cannot fully explain the highly aggressive nature of, and poor prognosis associated with, tumors with a low level of p27. To identify other mechanisms by which down-regulation of p27 expression might promote malignancy, we established a human cell line with a reduced level of p27 expression through targeted disruption of the *p27* gene in HCT116 colon carcinoma cells and then examined the effects of p27 deficiency in these cells on gene expression. We found that expression of the gene for G protein-coupled receptor 48 (GPR48) was increased in the p27<sup>+/-</sup> cells.

GPR48, also known as leucine-rich repeat (LRR)-containing G protein-coupled receptor 4 (LGR4), is a member of the G protein-coupled receptor (GPCR) family of proteins, but its biological function is unclear (11, 12). The GPCR family comprises proteins with seven transmembrane domains that function as the receptors for various classes of ligand, including peptide hormones and chemokines (13), and which are major targets for pharmaceutical development (14). Several GPCRs, including thyroid-stimulating hormone receptor and chemokine (C-X-C) receptor 4, have also been found to contribute to carcinogenesis (15). GPR48 is composed of a large NH<sub>2</sub>-terminal extracellular domain containing 18 LRRs, the seven membrane-spanning segments, and a COOH-terminal intracellular domain (11, 12). Although it is structurally similar to receptors for gonadotropins and thyroid-stimulating hormone, GPR48 is currently classified as an orphan receptor because its ligand has not been identified. However, GPR48 knockout mice were shown to manifest intrauterine growth retardation and renal development (16, 17).

We have now identified *GPR48* as a gene whose expression is up-regulated in p27-deficient HCT116 cells, and forced expression of GPR48 was found to increase the invasive and metastasis potential of HCT116 cells. Furthermore, GPR48 expression was inversely correlated with the expression of p27 in human colon carcinomas and was significantly associated with lymph node metastasis of these tumors. Our results suggest that GPR48 contributes to tumor invasiveness and metastasis.

Note: Supplementary data for this article are available at Cancer Research Online (<http://cancerres.aacrjournals.org/>).

Y. Gao and K. Kitagawa contributed equally to this study.

Competing interests statement: The authors declare that they have no competing financial interests.

Requests for reprints: Masatoshi Kitagawa, Department of Biochemistry 1, Hamamatsu University School of Medicine, 1-20-1 Handayama, Hamamatsu 431-3192, Japan. Phone: 81-53-435-2322; Fax: 81-53-435-2322; E-mail: kitamasa@hama-med.ac.jp.

©2006 American Association for Cancer Research.

doi:10.1158/0008-5472.CAN-06-2629

## Materials and Methods

**Cell culture and establishment of stable transformants.** Primary mouse embryonic fibroblasts (MEF) were obtained from embryos at 13.5 days after coitum by standard procedures (18–20). MEFs and all cell lines were cultured under a humidified atmosphere of 5% CO<sub>2</sub> at 37°C in DMEM supplemented with 10% fetal bovine serum, penicillin (100 units/mL), and streptomycin (100 µg/mL). GPR48 and Skp2 cDNAs were generated by reverse transcription-PCR (RT-PCR) from HeLa cell mRNA and subcloned into pcDNA4 (Invitrogen, San Diego, CA), and the resulting plasmids were introduced into HCT116 cells by transfection with the FuGene reagent (Roche, Indianapolis, IN). Stable transformants were selected by culture in the presence of zeocin (400 µg/mL).

**Targeted disruption of the p27 gene in HCT116 cells.** The targeting vector contained about 9 kb of p27 intron sequences and polyadenylate [poly(A)]-less G418-resistant gene substituted for p27 coding region. Translation of *neo* mRNA was thus dependent on integration of the vector upstream of the poly(A) sequence of the p27 gene in HCT116 cell line that has also been used previously to generate somatic knockout cells (21). HCT116 cells were transfected with the targeting vector with the use of the Lipofectamine reagent (Invitrogen), and stable transformants were selected with G418 (600 µg/mL). The resulting clones were screened for homologous recombinants by PCR analysis of genomic DNA. Only one clone among 464 G418-resistant colonies screened proved to be heterozygous for the p27 gene. This finding was confirmed by Southern blot analysis (data not shown).

**Microarray analysis.** Gene expression was compared between p27<sup>-/-</sup> and parental HCT116 cells by DNA microarray analysis with Motorola CodeLink Bioarrays (Kurabo, Osaka, Japan).

**Quantitative RT-PCR analysis.** Total RNA was isolated from frozen tissue specimens or cultured cells with the use of an Isogen kit (Wako, Osaka, Japan), and was subjected to reverse transcription with random hexanucleotide primers and SuperScript Reverse Transcriptase II (Invitrogen). The resulting cDNA was subjected to real-time PCR with the LightCycler System and a QuantiTect SYBR Green PCR kit (Qiagen, Chatsworth, CA). The primer sequences were TGGGAATCTTTTCCTGTCTG and GAACACTGAGACAGTATGCC for Skp2, CAGTACCCAGTGAAGCCATT and TGTTGTCATCCAGCCACAGA for GPR48, AACGTGCGAGTGTCTAACGG and GCCGTGCTCCTCAGAGTTAGCC for p27, and ACTGCTCGGCCAA-TGGCAA and TGGGTGCTCTACGCAACCATCT for p57. The abundance of transcripts of interest was normalized by that of glyceraldehyde-3-phosphate dehydrogenase mRNA or 18S rRNA as an internal standard. At least three independent analyses were done for each sample and for each gene.

**Generation of antibodies to GPR48.** A peptide (CQEQLRLFLDL) based on the large NH<sub>2</sub>-terminal ectodomain of human GPR48 was chemically synthesized, conjugated with keyhole limpet hemocyanin, and injected into rabbits. Specific antibodies to GPR48 were purified from the resulting antiserum by affinity chromatography with the peptide antigen as described in Gao et al. (22).

**Immunoblot analysis.** Cell lysates were prepared with lysis buffer (23), fractionated by SDS-PAGE on an 8% gel, and subjected to immunoblot analysis with antibodies to p27 (Transduction Laboratories, Lexington, KY), to Skp2 (Zymed, South San Francisco, CA), to β-actin (Sigma, St. Louis, MO), to CDK4 (Transduction Laboratories), to tubulin (Sigma), or to X-press (Invitrogen). Immune complexes were detected with horseradish peroxidase-conjugated secondary antibodies (Promega, Madison, WI) and an enhanced chemiluminescence system (NEN, Boston, MA).

**RNA interference.** Knockdown vectors for GPR48 or p27 small interfering RNAs (siRNA) were constructed by introduction of the 345-CAGTACCCAGTGAAGCCAT-369 (NM\_018490) and 217-GTACGAGTGG-CAAGAGGTG-235 (X84849), respectively, into the pSuper RNA interference (RNAi) vector (Oligoengine, Seattle, WA). The resulting plasmids or the control vector were introduced into HeLa or HCT116 cells by transfection with the use of FuGene (Roche), and stable “knockdown” clones were selected with hygromycin (150 µg/mL).

**Luciferase reporter assay.** Cells (200,000 per well) cultured in six-well plates were transfected with the use of the GT-I reagent (Dojindo, Kumamoto, Japan) with 1 µg of the luciferase reporter plasmid based on

PGV-B (Wako) and with 250 ng of the CMV-β-gal plasmid, with or without 40 ng (or the indicated amount) of an expression vector for human E2F1 (a gift from Dr. E. Hara, Tokushima University, Tokushima, Japan). Cells were lysed 48 hours after transfection and assayed for luciferase and β-galactosidase activities, with the former being normalized by the latter.

**Chromatin immunoprecipitation assay.** HEK293 cells grown overnight in 100-mm dishes to 60% to 70% confluency were transfected with 1 µg of the promoter construct using the FuGene reagent (Roche). The untransfected 293 cells for analysis of endogenous *GPR48* gene and promoter-transfected 293 cells were cross-linked with formaldehyde and harvested, and chromatin immunoprecipitations with anti-E2F1 (Santa Cruz Biotechnology, Santa Cruz, CA) and control mouse IgG were done. The remainder of the procedure followed standard protocols for chromatin immunoprecipitation analysis described by Upstake. The resulting DNA was analyzed by PCR reactions with a forward primer 5′-CGAAGTACCCTTAAAGCCGTAGTT and a reverse primer 5′-AAACATCTGAGTGGGAGGTGACTA.

**In vitro cell invasion assay.** Cells (5 × 10<sup>4</sup> per well) were placed in the upper chamber of a 24-well Transwell apparatus containing Matrigel membranes (BD Biosciences, San Jose, CA), and the lower chamber was filled with 750 µL DMEM supplemented with 0.1% bovine serum albumin and fibronectin (10 µg/mL; Roche) as a chemoattractant. After incubation for 36 hours at 37°C, cells that had migrated to the lower surface of each membrane were stained with the use of a Diff-Quik kit (International Reagents, Kobe, Japan) and counted. Each experiment was done with triplicate wells and repeated thrice.

**In vivo tumor metastasis.** To estimate the metastatic ability of GPR48, we used two lung colonization models. Briefly, HCT116 cells were prepared as single-cell suspensions in sterile PBS at a concentration of 2 × 10<sup>7</sup> per mL, and a volume of 250 µL (5 × 10<sup>6</sup> cells) was s.c. injected into 6-week-old male athymic nude mice (BALB/c nu/nu; purchased from Seiken Co. Ltd., Tokyo, Japan). HeLa cells were prepared as mentioned above at a concentration of 5 × 10<sup>6</sup> per mL, and a volume of 200 µL (1 × 10<sup>6</sup> cells) was injected via the tail vein (i.v.) into 6-week-old male athymic nude mice. Animals were sacrificed on a days between 35 and 42. The lungs were excised, fixed in formalin overnight, and sectioned discontinuously into six portions. The 5-µm sections were immunostained with mouse anti-human cytokeratin monoclonal antibody (Santa Cruz Biotechnology). Metastatic deposits <0.2 mm were considered micrometastases.

**Patient characteristics and tissue specimens.** Specimens of colon carcinoma and paired normal mucosal tissue were obtained from 29 Japanese patients (19 men and 10 women) who received no therapy before surgery. The histopathologic grade of tumor differentiation was defined as described (24). The median age of the patients was 64.9 years (range, 42–88 years).

**Immunostaining.** For immunohistochemical analysis, formalin-fixed, paraffin-embedded sections (thickness = 5 µm) were depleted of paraffin, rehydrated, and irradiated in a microwave oven for 40 minutes in 10 mmol/L sodium citrate buffer (pH 6). The sections were then incubated with 0.3% H<sub>2</sub>O<sub>2</sub> in absolute methanol for 30 minutes to quench endogenous peroxidase activity before exposure to antibodies to p27 (Transduction Laboratories) or to GPR48 (Hokkaido System Science generated in the present study). Immune complexes were detected with biotin-conjugated secondary antibodies, streptavidin-conjugated horseradish peroxidase, and diaminobenzidine with the use of a kit (Histofine SAB kit, Nichirei, Tokyo, Japan). The sections were lightly counterstained with hematoxylin and mounted with a permanent mounting medium. For the evaluation of p27 expression, the number of stained nuclei was counted (25); at least 10 high-power fields were chosen randomly for scoring of the percentage of cells positive for p27 staining among 1,000 cells examined per section.

**Statistical analysis.** Data are presented as means ± SE, and the statistical significance of differences was assessed with Fisher's exact test. *P* < 0.05 was considered statistically significant.

## Results

**GPR48 expression is inversely related to p27 expression in HCT116 and MEF cells.** To examine the mechanism by which p27 down-regulation increases tumor malignancy, we studied the human colon carcinoma cell line HCT116, which possesses wild-type *p53*

and retinoblastoma protein (*pRB*) genes and in which p27 degradation seems to occur normally during the cell cycle. This cell line has also been used previously to generate somatic knockout cells (21). We subjected the *p27* gene in HCT116 cells to targeted disruption (Fig. 1A), resulting in the isolation of one heterozygous recombinant clone (*p27*<sup>+/-</sup>) as revealed by PCR analysis (Fig. 1B, lane 1). Immunoblot analysis showed that the abundance of p27 was markedly reduced in the *p27*<sup>+/-</sup> cell clone compared with that in the parental HCT116 cells (wild type), and in Skp2-15 cell clone compared with that of the clone transfected with the corresponding empty vector (Fig. 1C, *Vec.*). The stable transformants and heterozygous recombinant clone above were subjected to an *in vitro* assay of cell invasion. The invasive activity of *p27*<sup>+/-</sup> was increased compared with parental cells (Fig. 1D, *left*). Therefore, down-regulation of p27 enhanced carcinoma cell invasiveness. With the use of DNA microarray analysis, we then screened for genes that are expressed differentially in the *p27*<sup>+/-</sup> and parental HCT116 cells. We found 26 differentially expressed genes between *p27*<sup>+/-</sup> and their parental cells by the microarray

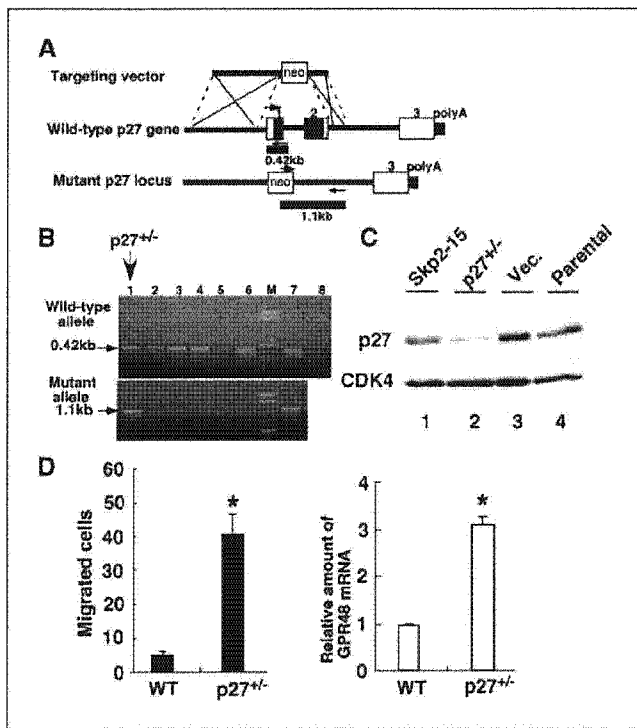


**Figure 1.** Up-regulation of *GPR48* gene expression in *p27*-deficient HCT116 cells. **A**, structure of the targeting vector, the human *p27* gene, and the mutant *p27* locus after homologous recombination. Numbered boxes, exons of the *p27* gene, with the coding regions shaded. Arrows, positions of PCR primers (sizes of the corresponding amplification products are shown). **B**, PCR-based screen for homologous recombination events in HCT116 cells transfected with the *p27*-targeting vector. Sizes of PCR products derived from the wild-type and mutant alleles are shown. Lane 1, *p27*<sup>+/-</sup> recombinant clone; lanes 2 to 6, non-recombinant clones; lane 7, positive control; lane 8, negative control; lane M, size markers. **C**, immunoblot analysis of p27 in HCT116 cells stably overexpressing Skp2 (Skp2-15) or transfected with the corresponding empty vector (*Vec.*), in the *p27*<sup>+/-</sup> recombinant clone, and in parental HCT116 cells (WT). The abundance of CDK4 was similarly probed as a loading control. **D**, the *p27*<sup>+/-</sup> recombinant clone (*p27*<sup>+/-</sup>) and parental HCT116 (WT) were assayed for invasive activity *in vitro* with a Transwell apparatus containing Matrigel membranes. The numbers of migrated cells were quantitated in three independent experiments (*left*). GPR48 mRNA in *p27*<sup>+/-</sup> and parental (WT) HCT116 cells were measured by quantitative RT-PCR analysis (*right*). \*, *P* < 0.01.

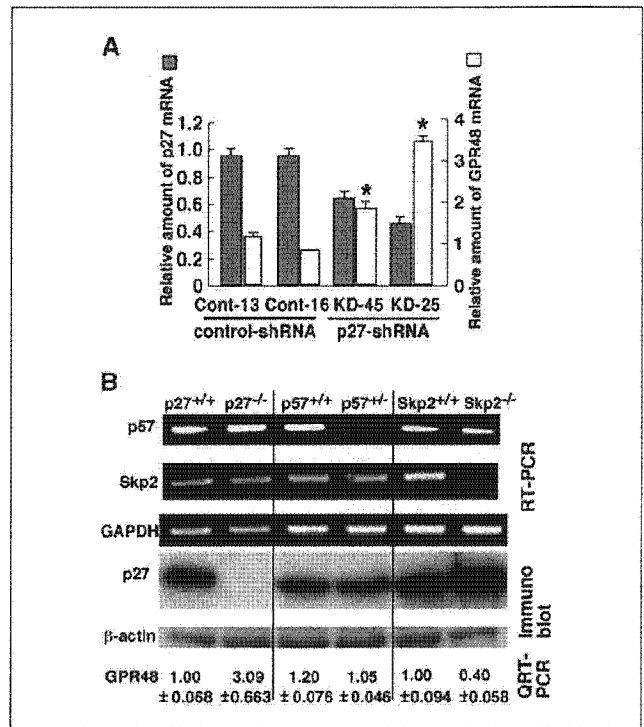


**Figure 2.** Inverse correlation of expression levels between GPR48 and p27. **A**, mRNA levels of both p27 and GPR48 in HCT116 clones stably transfected with a vector for p27 shRNA (p27-KD25 and p27-KD45) or with control siRNA plasmid vector (Cont-13 and Cont-16) were analyzed by quantitative RT-PCR. \*, *P* < 0.05. **B**, up-regulation of *GPR48* expression in *p27*<sup>-/-</sup> MEFs and its down-regulation in Skp2<sup>-/-</sup> MEFs. RT-PCR analysis of p57<sup>Kip2</sup> (female) and Skp2 mRNA and immunoblot analysis of p27 in MEFs of the indicated genotypes. Glyceraldehyde-3-phosphate dehydrogenase (*GAPDH*) mRNA and  $\beta$ -actin were analyzed as respective controls. Levels of GPR48 mRNA were measured by quantitative RT-PCR analysis.

analysis. Among these genes, 22 were down-regulated, and 4 were up-regulated in *p27*<sup>+/-</sup> cells compared with the parental ones. We selected several genes that could have potential to modulate signal transduction or cell motility or adhesion. We then did quantitative RT-PCR analyses of these genes to confirm the results of microarray analysis. Thus, we found that expression of the gene for GPR48 was reproducibly increased in the *p27*<sup>+/-</sup> HCT116 (Fig. 1D, *right*). We confirmed that the abundance of GPR48 mRNA in HCT116 cell lines stably expressing p27-shRNA was increased compared with that in control lines transfected with control short hairpin RNA (shRNA) plasmid vector (Fig. 2A). Moreover, Skp2-overexpressing cell lines with low p27 also showed an increased abundance of GPR48 mRNA (data not shown). The ligand and cellular functions of GPR48 are unknown. Because GPR48 knockout mice were shown to manifest intrauterine growth retardation and renal development (16, 17), we presumed that GPR48 might be involved in cell motility or differentiation as well as developmental events. Therefore, we focused on GPR48.

The inverse relation apparent between the expression of p27 and that of GPR48 in HCT116 cells was confirmed by experiments with MEF derived from p27 knockout (*p27*<sup>-/-</sup>) mice (18), heterozygous p57<sup>Kip2</sup> knockout (*p57*<sup>+/-</sup>) mice (19), and Skp2 knockout (*Skp2*<sup>-/-</sup>) mice (ref. 20; Fig. 2B). The amount of GPR48 mRNA was increased in *p27*<sup>-/-</sup> MEFs compared with that in *p27*<sup>+/+</sup> MEFs, did not differ between *p57*<sup>+/-</sup> and *p57*<sup>+/+</sup> MEFs, and was reduced in *Skp2*<sup>-/-</sup>

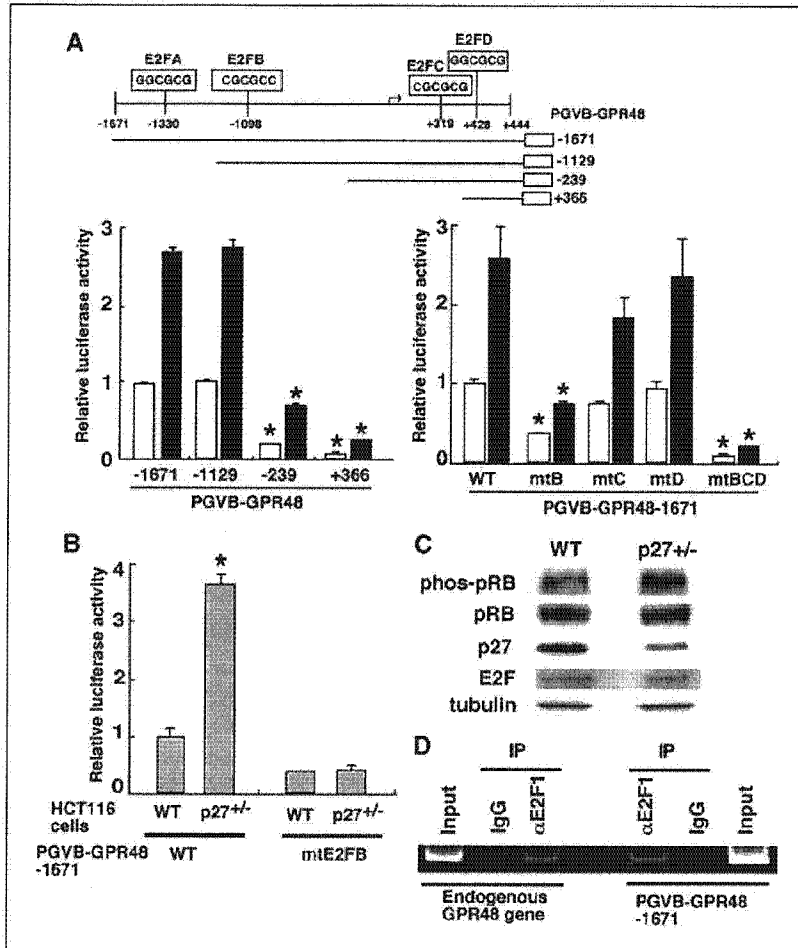


**Figure 3.** Activation of the *GPR48* promoter by E2F1. **A**, schematic representation of the human *GPR48* promoter-containing luciferase (*Luc*) reporter plasmids, showing the positions of putative E2F-binding sites. *Arrow*, transcription initiation site. The reporter plasmid pGVB-GPR48-1671 (WT), its deletion mutant plasmids (*left*), and its E2F site mutant plasmids (*right*) as indicated were cotransfected to HCT116 cells with (*closed column*) or without (*open column*) an expression vector for E2F1. Cells were subsequently lysed and assayed for luciferase activity. \*,  $P < 0.01$  versus values for pGVB-GPR48-1671 (WT). **B**, wild-type (WT) or p27<sup>+/−</sup> HCT116 cells were transfected with equimolar amounts of PGVB-GPR48-1671 or PGVB-GPR48-mtE2FB (*right*). E2FB site-dependent activation of *GPR48* promoter was observed in p27<sup>+/−</sup> HCT116 cells. \*,  $P < 0.01$  versus values for pGVB-GPR48-1671 (WT). **C**, phosphorylation of pRB in the wild-type (WT) and p27<sup>+/−</sup> HCT116 cells were examined for immunoblotting with anti-phospho-pRB antibody (*phos-pRB*) or indicated antibodies. **D**, binding of E2F1 to E2FB site was analyzed by chromatin immunoprecipitation assay using anti-E2F1 or a control IgG antibody in cells transfected without (*left*, for analysis of the endogenous *GPR48* gene) or with PGVB-GPR48-1671 (*right*). PCR amplification products of immunoprecipitates using *GPR48* promoter primers were analyzed by 5% acrylamide gel electrophoresis.

MEFs relative to that in Skp2<sup>+/+</sup> MEFs. Together, these results suggested that p27 negatively affects expression of the *GPR48* gene.

**Activation of the *GPR48* promoter by E2F1.** To investigate the mechanism by which p27 deficiency results in increased *GPR48* expression, we first examined the promoter of *GPR48* for transcription factor binding sites with the use of the Tf-binding database.<sup>7</sup> We identified four putative E2F-binding sites (E2FA, E2FB, E2FC, and E2FD) in the *GPR48* promoter (Fig. 3A, top). We speculated that the transactivation activity of E2F might be increased as a result of down-regulation of p27 expression, given that an increase in CDK activity has been shown to activate E2F in the pRB pathway (26). To determine whether E2F1 activates the *GPR48* promoter, we did a luciferase reporter assay with the plasmid PGVB-GPR48-1671, which contains nucleotides -1671 to +444 (NM\_018490; relative to the transcription start site) of human *GPR48* and with various mutants thereof (Fig. 3A). The *GPR48* promoter was activated by E2F1 in a concentration-dependent manner in transfected HCT116 cells (Supplementary Fig. S1). The luciferase activity of cells transfected with the plasmid PGVB-GPR48-239 in the absence or presence of the E2F1 plasmid was greatly reduced compared with the corresponding values obtained with PGVB-GPR48-1671 (Fig. 3A, left). Moreover,

mutation of the E2FB site (mtE2FB) or of E2FB, E2FC, and E2FD sites (mtE2FBCD) resulted in a marked reduction in both basal and E2F1-dependent transcriptional activity of the *GPR48* promoter (Fig. 3A, right). These results suggested that the E2FB site is indispensable for basal and E2F1-dependent activity of the *GPR48* promoter. Next, we examined whether *GPR48* promoter activity was enhanced in p27<sup>+/−</sup> cells using the reporter assay. The luciferase activity derived from PGVB-GPR48-1671 was substantially greater in p27<sup>+/−</sup> cells than in the wild-type cells, whereas that derived from PGVB-GPR48-mtE2FB was low and similar in cells of both genotypes (Fig. 3B). Moreover, to address the mechanisms of activation of *GPR48* promoter in p27<sup>+/−</sup> cells, E2F and RB protein were analyzed by Western blotting. We found that phosphorylation of RB protein was increased in p27<sup>+/−</sup> HCT116 cells (Fig. 3C). Moreover, we examined whether E2F1 protein actually bound to E2FB site using chromatin immunoprecipitation assay. As shown in Fig. 3D, immunoprecipitates with anti-E2F1 from cells with or without transfection of PGVB-GPR48-1671 reporter plasmid were contained with E2FB site on the *GPR48* promoter. The result suggests that E2F1 actually bound to endogenous as well as exogenous the *GPR48* promoter. These findings thus suggested that the up-regulation of *GPR48* expression induced by deficiency of p27 is mediated by an increase in the transactivation activity of E2F1, which may be free from RB protein.

<sup>7</sup> <http://www.ifti.org/TfSitescan/>.

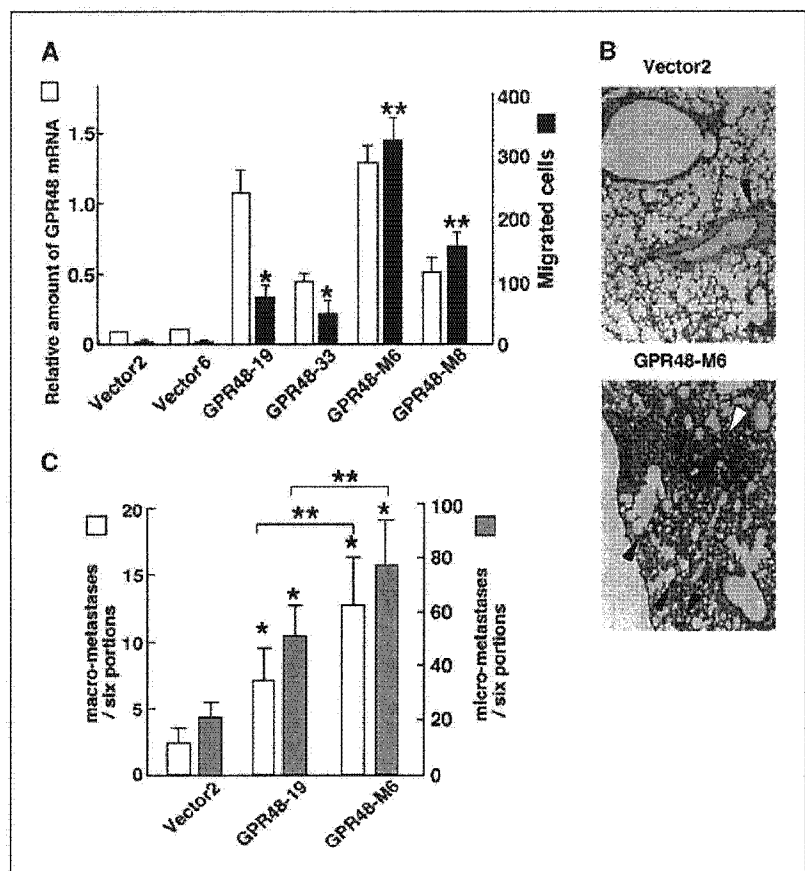
**GPR48 increases the invasive activity of HCT116 cells.** As described above, the invasive activity of p27<sup>-/-</sup> was increased compared with parental cells (Fig. 1D). Our findings suggested that GPR48 might be important in metastasis of human tumors. To determine whether GPR48 affects the invasive activity of HCT116 cells, we generated lines stably transfected with expression vectors for wild-type GPR48. There was no significant difference in growth rate between clones expressing wild-type GPR48 and control clones (see Supplementary Fig. S2). Comparing the structures of the constitutively active mutants of the luteinizing hormone and thyrotropin receptors with that of the related protein GPR48, we have successfully constructed GPR48-T755I, a constitutively active mutant of human GPR48 recently (22). Ectopic expression of GPR48-T755I into HEK293 cells enhanced basal cyclic AMP (cAMP) levels compared with that of wild-type GPR48 (Supplementary Fig. S3). HCT116 cell clones stably expressing GPR48-T755I (GPR48-M6 and GPR48-M8) were about 3-fold higher cAMP levels than wild-type GPR48-expressing clones (22). As shown in Fig. 4A, the invasive activity of cell clones expressing wild-type GPR48 (GPR48-19 and GPR48-33) was significantly higher than that of those transfected with the corresponding empty vector (Vector2 and Vector6). The constitutively active mutant GPR48-T755I was more effective on the cell invasiveness (GPR48-M6 and GPR48-M8). These results thus indicate that GPR48 increases the invasive potential of colon carcinoma cells.

**Acceleration of lung metastasis by ectopic expression of GPR48 in HCT116.** To examine whether the invasive effect of

GPR48 *in vitro* has a physiologic relevance *in vivo*, we injected HCT116 clones into nude mice s.c. and compared the occurrence of pulmonary colonization in GPR48-overexpressing clones (GPR48-19 and GPR48-M6; see Fig. 4A) versus corresponding vector-transfected HCT116 clones (Vector2) after a period of 6 weeks. To confirm that these metastatic lesions had originated from injected cells, we check these samples by immunostaining with human-specific cytokeratin (Fig. 4B). We defined that metastatic deposits <0.2 mm were considered micrometastases, and >0.2 mm were considered macrometastases. We used eight mice for each lung metastasis assay and did statistical analyses. Interestingly, overexpression of wild-type GPR48 significantly increased the number of macrometastasis and micrometastasis in lung compared with vector-transfected cells (Fig. 4B and C), whereas there was no significant difference in primary s.c. tumor weight between clones overexpressing wild-type or mutant GPR48 and control clones (Supplementary Fig. S4). Moreover, constitutive active mutant of GPR48 (GPR48-M6) was more effective on metastasis than wild-type GPR48 (GPR48-19). The results suggest that enhanced expression of GPR48 promotes not only invasiveness but also metastasis.

**Depletion of endogenous GPR48 reduces the invasion potential of HeLa cells.** Quantitative RT-PCR analysis showed that GPR48 expression was quite low in parental HCT116 cells, as shown in Supplementary Fig. S5. Because the invasive activity of HCT116 was also low (Fig. 1D and Fig. 4A), we thought that HCT116 was also suitable to evaluate the effects of GPR48 overexpression on invasiveness and metastasis. To confirm the relation

**Figure 4.** Effects of GPR48 on the invasive activity of human carcinoma cell lines. **A**, HCT116 cell clones stably transfected either with expression vectors for wild-type GPR48 (GPR48-19 and GPR48-33) or the constitutively active mutant GPR48-T755I (GPR48-M6 and GPR48-M8) or with the corresponding empty vector (Vector2 and Vector6) were assayed for invasive activity *in vitro* with a Transwell apparatus containing Matrigel membranes. The numbers of migrated cells were quantitated in three independent experiments (closed column). The various stably transfected HCT116 cell clones were subjected to quantitative RT-PCR analysis of GPR48 (open column). \*,  $P < 0.05$ , \*\* $P < 0.01$ . **B**, acceleration of lung metastasis by ectopic expression of GPR48 in HCT116. HCT116 cell clones, vector2, GPR48-19, and GPR48-M6 were s.c. injected into nude mice ( $n = 8$ ). Five weeks after injection, mice were sacrificed. Weights of their s.c. primary tumors were unchanged as indicated in Supplementary Fig. S4. Representative immunostainings with anti-human cytokeratin monoclonal antibody for macrometastasis (open arrowhead) and micrometastasis (closed arrowheads) in the lung. Original magnification,  $\times 200$ . **C**, quantification of macro and micro lung metastasis of Vector2, GPR48-19, and GPR48-M6 cells. \*,  $P < 0.01$ , GPR48-19 or GPR48-M6 versus Vector2; \*\*,  $P < 0.05$ , GPR48-M6 versus GPR48-19.





between GPR48 expression and cell invasion potential, we used RNAi to deplete endogenous GPR48 of HeLa and Lewis lung carcinoma (mouse LLC) cells (Fig. 5A). Expressions of GPR48 in HeLa and LLC cells were 17- and 3.7-fold, respectively, higher than that in HCT116 cells (Supplementary Fig. S5). Moreover, these two cells showed high invasive potential as shown in Fig. 5B and C, respectively. Therefore, we thought that HeLa and LLC cells were suitable to evaluate the effects of down-regulation of endogenous GPR48 on invasiveness and metastasis. We found that siRNA against GPR48 (GPR48-si450) remarkably inhibited invasion of HeLa cells. Moreover, we established HeLa cell clones stably expressing GPR48 shRNA (GPR48-KD1 and GPR48-KD4). The depletion of GPR48 was confirmed by immunofluorescence (Supplementary Fig. S6A) and quantitative RT-PCR (Fig. 5B, *open column*) analyses; the amount of GPR48 mRNA was reduced by >80% in these clones compared with that in control clones transfected with control shRNA plasmid vector (Cont-1 and Cont-3). The invasive activity of both GPR48-KD1 and GPR48-KD4 clones was significantly reduced compared with that of the control clones (Fig. 5B, *closed column*; Supplementary Fig. S6A). The depletion of endogenous GPR48 in LLC cell clones stably expressing GPR48 shRNA also diminished invasive activities of both GPR48-KD3 and GPR48-KD24 clones (Fig. 5C). These results thus confirmed that endogenous GPR48 is involved in the invasive potential of cancer cells.

**Depletion of endogenous GPR48 suppresses lung metastasis.**

Next, we injected GPR48-depleted HeLa cells (GPR48-KD4; see Fig. 5B) or the control clone (Cont-1) via the tail vein of nude mice. After 5 weeks, we found that GPR48-depleted HeLa cells have significantly reduced pulmonary colonization compared with control cells (Supplementary Fig. S6B and C). Moreover, we s.c. injected GPR48-depleted LLC cells (GPR48-KD3 and GPR48-KD4; see Fig. 5C) or the control clone (Cont-5 and Cont-6) into mice. Lung metastasis potencies of LLC cells were significantly decreased by stably expressing GPR48 shRNA (Fig. 5D), whereas there was no significant difference in primary tumor weight between GPR48-depleted and control clones (data not shown). These data suggest that GPR48 contributes to metastasis of carcinoma *in vivo* as well as *in vitro*. Because metastasis is a multi-step process, we investigated whether GPR48 affected angiogenesis using immunohistochemical analyses with anti-CD34 antibodies. Although further experiments are required, there was no significant effect of GPR48 expression on angiogenesis in the primary tumors (data not shown). Moreover, we did terminal deoxynucleotidyl transferase-mediated nick-end labeling assay with the primary tumors and found no significant effect of GPR48 expression on apoptosis in the primary tumors (data not shown).

**Clinical relevance of GPR48 expression in colon carcinoma.**

To evaluate clinical relevance between GPR48 expression and metastasis, we next measured the amount of GPR48 mRNA in

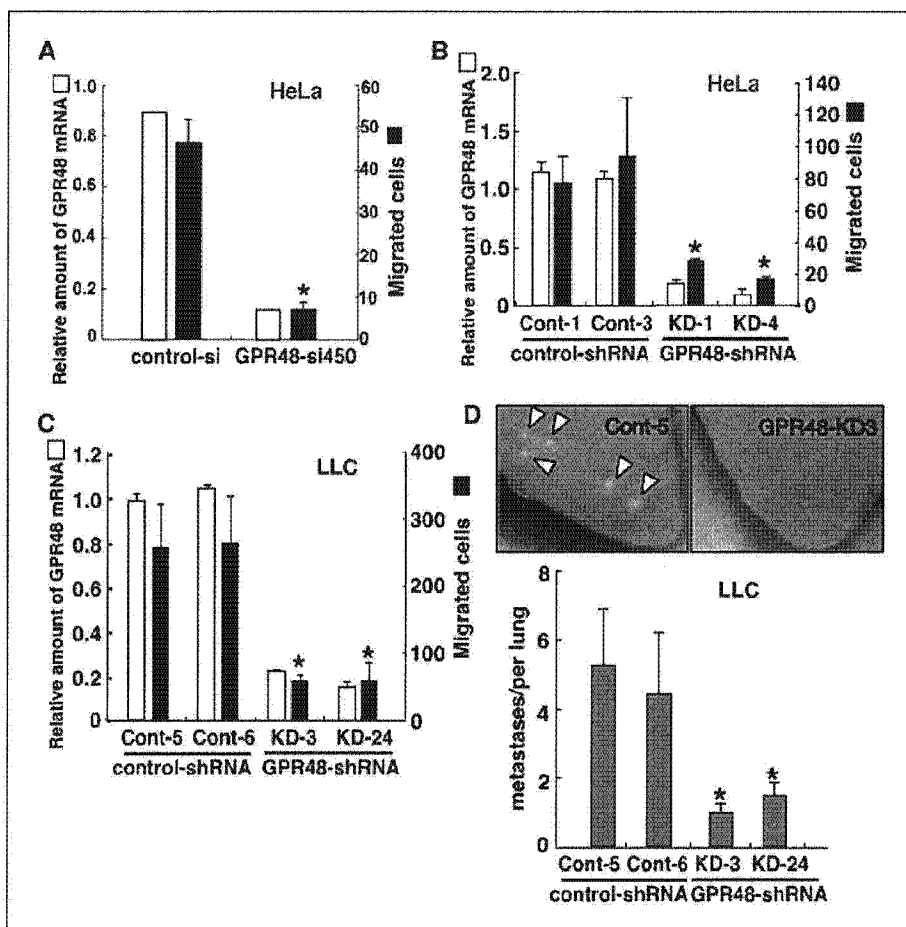


**Figure 5.** Effects of depletion of endogenous GPR48 on invasiveness and metastasis. **A**, HeLa cells were treated with siRNA-oligos (200 nmol/L) specific for GPR48 (GPR48-si450) or with nonspecific control (control-si) for 48 hours, and then they were assayed for invasive activity *in vitro* with a Transwell apparatus containing Matrigel membranes (*closed column*). \*,  $P < 0.01$  versus values for control-si. Efficacies of GPR48 depletion were evaluated by quantitative RT-PCR analysis (*open column*). **B**, HeLa clones stably transfected with an expression vector for GPR48 shRNA (GPR48-KD1 and GPR48-KD4) or with the corresponding control shRNA plasmid vector (Cont-1 and Cont-3) were subjected to immunofluorescence analysis with anti-GPR48 antibody and quantitative RT-PCR analysis of GPR48 mRNA. The invasive activity of the various HeLa cell clones was assayed *in vitro*. Quantitative data. \*,  $P < 0.05$  versus values for Cont-1 or Cont-3. **C**, LLC cell clones stably transfected with an expression vector for GPR48 shRNA (GPR48-KD3 and GPR48-KD24) or with the corresponding control shRNA plasmid vector (Cont-5 and Cont-6) were subjected to quantitative RT-PCR analysis of GPR48 mRNA. The invasive activity of the indicated clones was assayed *in vitro*. Quantitative data. \*,  $P < 0.05$  versus values for Cont-5 or Cont-6. **D**, suppression of lung metastasis by depletion of GPR48. LLC cell clones, Cont-5, Cont-6, GPR48-KD3, and GPR48-KD24 in (C) were s.c. injected into mice ( $n = 8$ ). Four weeks after injection, mice were sacrificed. Representative photographs of pulmonary colonization (*open arrowheads*) were indicated (*top*). The pulmonary colonies were counted and subjected to statistical analysis (*bottom*). \*,  $P < 0.05$ .

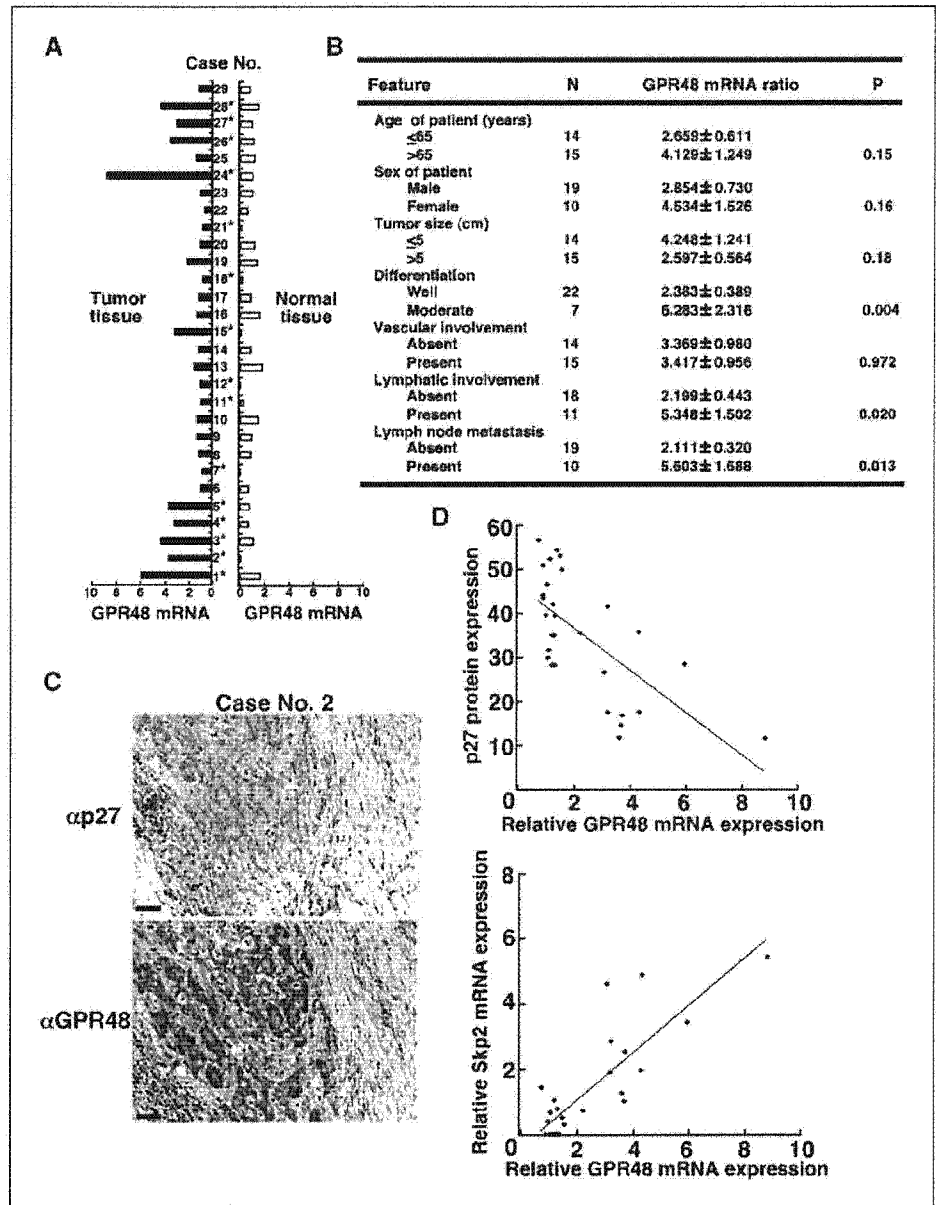


**Figure 6.** Expression of *GPR48* in human colon carcinoma. *A*, the amount of *GPR48* mRNA was determined in 29 specimens of human colon carcinoma and paired adjacent normal mucosal tissue. \*, cases in which the abundance of *GPR48* mRNA in the tumor tissue was more than twice that in the corresponding normal tissue. *B*, relation between the tumor/normal tissue ratio of *GPR48* mRNA abundance and clinicopathologic features of the 29 cases of colon carcinoma. *C*, representative immunohistochemical staining for p27 (*top*) and *GPR48* (*bottom*) in colon carcinoma tissue. Original magnification, ×200. Bar, 100 μm. *D*, relations between the amount of *GPR48* mRNA and either the proportion of cells expressing p27 ( $R^2 = 0.4445$ ,  $r = -0.667$ ,  $P < 0.0001$ ; *top*) or the amount of *Skp2* mRNA ( $R^2 = 0.7033$ ,  $r = 0.838$ ,  $P < 0.0001$ ; *bottom*) in the 29 specimens of human colon carcinoma.

surgical specimens of human colon carcinoma and paired adjacent normal mucosal tissue. The abundance of *GPR48* mRNA in the colon carcinoma tissue was more than twice that in the normal tissue for 15 (52%) of the 29 specimens examined (Fig. 6*A*). The mean amount of *GPR48* mRNA for all tumor samples was significantly greater than that for all normal tissue samples (data not shown). The potential relation between *GPR48* expression and clinicopathologic features of colon carcinoma was also examined (Fig. 6*B*). The extent of the up-regulation of *GPR48* mRNA in tumors was greater in moderately differentiated carcinomas than in well-differentiated carcinomas. The extent of the increase in the amount of *GPR48* mRNA was also significantly greater in tumors with lymphatic involvement or with lymph node metastasis than in the corresponding tumors without such involvement or metastasis. No significant differences in *GPR48* expression among tumors were apparent with regard to age or sex of the patient, tumor size, or

vascular involvement. These data suggested that up-regulation of *GPR48* expression might contribute to lymphatic invasion or metastasis of human colorectal carcinoma.

**Relation among p27, *Skp2*, and *GPR48* expression in colon carcinoma.** We investigated the relation between the abundance of p27 and *GPR48* in the 29 specimens of colon carcinoma. As shown in Fig. 6*C*, as a representative data using immunohistochemical analysis, the amounts of the two proteins seemed to be inversely related. Quantitation of the proportion of tumor cells expressing p27 in each specimen indeed revealed an inverse correlation with the abundance of *GPR48* mRNA (Fig. 6*D, top*). In contrast, the amount of *Skp2* mRNA was directly correlated with that of *GPR48* mRNA in the tumor samples (Fig. 6*D, bottom*). These results indicated that *GPR48* expression was significantly associated with lymph node metastasis and inversely correlated with p27 expression in human colon carcinomas.

## Discussion

Given that p27 is an important negative regulator of the cell cycle, the major effect of a decrease in the expression of p27 has been thought to be an increase in the rate of cell growth. Pathologic studies have revealed that the abundance of p27 in tumors is inversely correlated with malignancy and is associated with clinical prognosis of human cancers (9). However, the biological mechanism underlying the increased malignancy of p27-deficient tumors has not been shown. The expression of Skp2, a component of an SCF-type ubiquitin ligase that targets p27 for degradation, is associated with poor prognosis in several human cancers (9, 10). Skp2 regulates the degradation not only of p27 but also of p130 (9), c-Myc (27), p57<sup>Kip2</sup> (19), p21<sup>Cip1</sup> (28), and Cdt1 (9). We therefore subjected the p27 gene of the HCT116 human colon carcinoma cell line to targeted disruption to provide a model for carcinoma cells with a low level of p27 expression. We found that expression of the GPR48 gene was increased not only in p27<sup>+/-</sup> HCT116 cells but also in HCT116 cells depleted of p27 by RNAi and in p27<sup>-/-</sup> MEFs, and that the expression of p27 and the abundance of GPR48 mRNA were inversely correlated in clinical specimens of colon carcinoma. Moreover, we showed that GPR48 increases the invasive or potential of cancer cells *in vitro*, promotes metastasis *in vivo* and GPR48 expression, was associated with lymphatic metastasis of colon carcinoma. There was no difference in *in vitro* cell growth (Supplementary Fig. S2; data not shown), *in vivo* primary tumor growth (Supplementary Fig. S4), and soft agar colony formation (data not shown) regardless of GPR48 expression. These data strongly suggest that GPR48 enhances carcinoma cell invasiveness and metastasis but not cell proliferation and cell transformation. GPR48 is an orphan receptor of which function and signal transduction have not been clear. Although further study is required, our study shows that up-regulation of GPR48 induced by p27-down-regulation promotes tumor cell invasion.

We identified four putative E2F-binding sites in the upstream regulatory region of *GPR48* and showed that these sites mediate transcriptional induction of *GPR48* in response to down-regulation of p27 expression. A decrease in the abundance of p27 is thought to result in activation of G<sub>1</sub> cyclin-CDK complexes, phosphorylation and inactivation of pRB, and abrogation of inhibition of E2F by pRB (26). The resulting increase in E2F activity might thus underlie the transcriptional activation of *GPR48* apparent in p27-deficient cells.

Previous studies have suggested that p27 inhibits the motility of various cell types (29–31). Cytoplasmic p27 has also been shown to

inhibit stathmin-mediated microtubule destabilization by binding to stathmin and thereby inhibits sarcoma cell migration (32). Skp2 also promotes the formation of filopodia and cell motility (33). On the other hand, p27 and other members of the Cip-Kip family have been shown to inhibit the Rho signaling pathway that underlies reorganization of the actin cytoskeleton and cell migration (34, 35). The increase in cancer cell invasiveness induced by degradation of p27 may thus be mediated by CDK-independent effects on microtubules and actin filaments as well as by CDK-dependent transcriptional activation of *GPR48* via unknown mechanisms. It has been reported that some GPCR, such as endothelin receptor, linked Rho family via Gα12 and RhoGEF to promote tumor metastasis (36, 37). GPR48 is an orphan GPCR of which function has not been elucidated except for stimulation of cAMP production by its activation as recently reported by us (22). We will investigate whether GPR48 also links Rho family GTPase and regulate actin filament organization promoting cell motility.

Whereas expression of GPR48 in normal colon tissue was low, it was markedly up-regulated in colon carcinoma. Moreover, a high level of GPR48 expression was associated with lymph node metastasis and lymphatic involvement. GPR48 is thus a potential marker for prediction of metastasis or poor prognosis in colorectal carcinoma. Depletion of endogenous GPR48 by RNAi resulted in a marked decrease lung metastasis in mouse models as well as in the invasive activity of HeLa and LLC cells. A similar down-regulation of GPR48 expression induced by a specific siRNA or antisense oligonucleotides *in vivo* might thus prevent metastasis of colorectal carcinoma or other tumors. Human type neutralizing monoclonal antibody against GPR48 may be clinically applicable for prevention of metastasis. Identification of the native ligand for GPR48 should also facilitate the development of GPR48-based therapeutics.

## Acknowledgments

Received 7/17/2006; revised 9/23/2006; accepted 10/10/2006.

**Grant support:** Ministry of Education, Science, Sports, Culture, and Technology of Japan (M. Kitagawa and K. Kitagawa); Grant-in-aid for Third-Term Comprehensive Control Research for Cancer from the Ministry of Health, Labor, and Welfare (M. Kitagawa); and COE program of Hamamatsu University School of Medicine funded by the Ministry of Education, Science, Sports, Culture, and Technology (M. Kitagawa).

The costs of publication of this article were defrayed in part by the payment of page charges. This article must therefore be hereby marked *advertisement* in accordance with 18 U.S.C. Section 1734 solely to indicate this fact.

We thank E. Hara for plasmids; S. Suzuki, T. Abe, K. Komiya, E. Murata, D. Hiraoka, and D. Ueno for technical assistance; and K. Nishimori, S. Kato, T. Takeuchi, H. Kobayashi, H. Ihara, and members of our laboratories for helpful discussions.

## References

- Porter PL, Malone KE, Heagerty PJ, et al. Expression of cell-cycle regulators p27Kip1 and cyclin E, alone and in combination, correlates with survival in young breast cancer patients. *Nat Med* 1997;3:222–5.
- Catzavelos C, Bhattacharya N, Ung YC, et al. Decreased levels of the cell-cycle inhibitor p27Kip1 protein: prognostic implications in primary breast cancer. *Nat Med* 1997;3:227–30.
- Fredersdorf S, Burns J, Milne AM, et al. High level expression of p27(kip1) and cyclin D1 in some human breast cancer cells: inverse correlation between the expression of p27(kip1) and degree of malignancy in human breast and colorectal cancers. *Proc Natl Acad Sci U S A* 1997;94:6380–5.
- Slingerland J, Pagano M. Regulation of the cdk inhibitor p27 and its deregulation in cancer. *J Cell Physiol* 2000;183:10–7.
- Sherr CJ, Roberts JM. CDK inhibitors: positive and negative regulators of G1-phase progression. *Genes Dev* 1999;13:1501–12.
- Sutterluty H, Chatelain E, Marti A, et al. p45SKP2 promotes p27Kip1 degradation and induces S phase in quiescent cells. *Nat Cell Biol* 1999;1:207–14.
- Kamura T, Hara T, Kotoshiba S, et al. Cytoplasmic ubiquitin ligase KPC regulates proteolysis of p27(Kip1) at G<sub>1</sub> phase. *Nat Cell Biol* 2004;6:1229–35.
- Loda M, Cukor B, Tam SW, et al. Increased proteasome-dependent degradation of the cyclin-dependent kinase inhibitor p27 in aggressive colorectal carcinomas. *Nat Med* 1997;3:231–4.
- Bloom J, Pagano M. Deregulated degradation of the cdk inhibitor p27 and malignant transformation. *Semin Cancer Biol* 2003;13:41–7.
- Gstaiger M, Jordan R, Lim M, et al. Skp2 is oncogenic and overexpressed in human cancers. *Proc Natl Acad Sci U S A* 2001;98:5043–8.
- Hsu SY, Liang SG, Hsueh AJ. Characterization of two LGR genes homologous to gonadotropin and thyrotropin receptors with extracellular leucine-rich repeats and a G protein-coupled, seven-transmembrane region. *Mol Endocrinol* 1998;12:1830–45.
- Loh ED, Broussard SR, Liu Q, et al. Chromosomal localization of GPR48, a novel glycoprotein hormone receptor like GPCR, in human and mouse with radiation hybrid and interspecific backcross mapping. *Cytogenet Cell Genet* 2000;89:2–5.
- Schoneberg T, Schultz G, Gudermann T. Structural basis of G protein-coupled receptor function. *Mol Cell Endocrinol* 1999;151:181–93.
- Brink CB, Harvey BH, Bodenstein J, Venter DP, Oliver DW. Recent advances in drug action and therapeutics: relevance of novel concepts in G-protein-coupled receptor and signal transduction pharmacology. *Br J Clin Pharmacol* 2004;57:373–87.
- Dhanasekaran N, Heasley LE, Johnson GL. G




- protein-coupled receptor systems involved in cell growth and oncogenesis. *Endocr Rev* 1995;16:259-70.
16. Mazerbourg S, Bouley DM, Sudo S, et al. Leucine-rich repeat-containing G protein-coupled receptor 4 null mice exhibit intrauterine growth retardation associated with embryonic and perinatal lethality. *Mol Endocrinol* 2004;18:2241-54.
  17. Kato S, Matsubara M, Matsuo T, et al. Leucine-rich repeat-containing G protein-coupled receptor-4 (LGR4, Gpr48) is essential for renal development in mice. *Nephron Exp Nephrol* 2006;104:e63-75.
  18. Nakayama K, Ishida N, Shirane M, et al. Mice lacking p27(Kip1) display increased body size, multiple organ hyperplasia, retinal dysplasia, and pituitary tumors. *Cell* 1996;85:707-20.
  19. Kamura T, Hara T, Kotoshiba S, et al. Degradation of p57Kip2 mediated by SCFSkp2-dependent ubiquitylation. *Proc Natl Acad Sci U S A* 2003;100:10231-6.
  20. Nakayama K, Nagahama H, Minamishima YA, et al. Targeted disruption of Skp2 results in accumulation of cyclin E and p27(Kip1), polyploidy and centrosome overduplication. *EMBO J* 2000;19:2069-81.
  21. Bunz F, Dutriaux A, Lengauer C, et al. Requirement for p53 and p21 to sustain G<sub>2</sub> arrest after DNA damage. *Science* 1998;282:1497-501.
  22. Gao Y, Kitagawa K, Shimada M, et al. Generation of a constitutively active mutant of human GPR48/LGR4, a G-protein-coupled receptor. *Hokkaido Igaku Zasshi* 2006;81:101-5.
  23. Uchida C, Miwa S, Kitagawa K, et al. Enhanced Mdm2 activity inhibits pRB function via ubiquitin-dependent degradation. *EMBO J* 2005;24:160-9.
  24. Hamilton PW, Allen DC, Watt PC, Patterson CC, Biggart JD. Classification of normal colorectal mucosa and adenocarcinoma by morphometry. *Histopathology* 1987;11:901-11.
  25. Inui N, Kitagawa K, Miwa S, et al. High expression of Cks1 in human non-small cell lung carcinomas. *Biochem Biophys Res Commun* 2003;303:978-84.
  26. Kamb A. Cell-cycle regulators and cancer. *Trends Genet* 1995;11:136-40.
  27. von der Lehr N, Johansson S, Wu S, et al. The F-box protein Skp2 participates in c-Myc proteasomal degradation and acts as a cofactor for c-Myc-regulated transcription. *Mol Cell* 2003;11:1189-200.
  28. Bornstein G, Bloom J, Sitry-Shevah D, Nakayama K, Pagano M, Hershko A. Role of the SCFSkp2 ubiquitin ligase in the degradation of p21Cip1 in S phase. *J Biol Chem* 2003;278:25752-7.
  29. Sun J, Marx SO, Chen HJ, Poon M, Marks AR, Rabbani LE. Role for p27(Kip1) in vascular smooth muscle cell migration. *Circulation* 2001;103:2967-72.
  30. Goukassian D, Diez-Juan A, Asahara T, et al. Overexpression of p27(Kip1) by doxycycline-regulated adenoviral vectors inhibits endothelial cell proliferation and migration and impairs angiogenesis. *FASEB J* 2001;15:1877-85.
  31. Daniel C, Pipin J, Shankland SJ, Hugo C. The rapamycin derivative RAD inhibits mesangial cell migration through the CDK-inhibitor p27KIP1. *Lab Invest* 2004;84:588-96.
  32. Baldassarre G, Belletti B, Nicoloso MS, et al. p27(Kip1)-stathmin interaction influences sarcoma cell migration and invasion. *Cancer Cell* 2005;7:51-63.
  33. Masuda TA, Inoue H, Sonoda H, et al. Clinical and biological significance of S-phase kinase-associated protein 2 (Skp2) gene expression in gastric carcinoma: modulation of malignant phenotype by Skp2 overexpression, possibly via p27 proteolysis. *Cancer Res* 2002;62:3819-25.
  34. Besson A, Gurian-West M, Schmidt A, Hall A, Roberts JM. p27Kip1 modulates cell migration through the regulation of RhoA activation. *Genes Dev* 2004;18:862-76.
  35. Denicourt C, Dowdy SF. Cip/Kip proteins: more than just CDK inhibitors. *Genes Dev* 2004;18:851-5.
  36. Titus B, Frierson HF, Jr., Conaway M, et al. Endothelin axis is a target of the lung metastasis suppressor gene RhoGD12. *Cancer Res* 2005;65:7320-7.
  37. Bhattacharya AV, Babwab AV, Ferguson SSG. Small GTP-binding protein-coupled receptors. *Biochem Soc Trans* 2004;32:1040-4.

## Transcriptional up-regulation of MMPs 12 and 13 by asbestos occurs via a PKC $\delta$ -dependent pathway in murine lung

Arti Shukla,\* Trisha F. Barrett,\* Keiichi I. Nakayama,<sup>†</sup> Keiko Nakayama,<sup>†</sup> Brooke T. Mossman,\* and Karen M. Lounsbury\*<sup>1</sup>

\*Departments of Pathology and Pharmacology, University of Vermont, Burlington, Vermont, USA; and <sup>†</sup>Department of Molecular Genetics, Medical Institute of Bioregulation, Kyushu University, Fukuoka, Japan

 To read the full text of this article, go to <http://www.fasebj.org/cgi/doi/10.1096/fj.05-4554fje>

### SPECIFIC AIMS

Matrix metalloproteases (MMPs) play an important role in lung remodeling in response to various environmental agents; however, their role in asbestos-induced lung diseases remains unexplored. In this study we tested the hypothesis that asbestos causes transcriptional up-regulation of various MMPs via a PKC $\delta$ -dependent pathway both in vitro and in vivo. Moreover, we hypothesized that asbestos-induced MMPs were regulated by multiple signaling pathways and governed extracellular signal-regulated kinase (ERK1/2) phosphorylation via epidermal growth factor receptor (EGFR) activation in epithelial cells.

### PRINCIPAL FINDINGS

#### 1. Asbestos exposure causes up-regulation of MMP mRNA levels in lungs that are reduced in PKC $\delta$ (-/-) mice

Oligonucleotide microarray analysis (Affymetrix) on RNA prepared from whole lungs of C57Bl/6 wild-type (WT) [PKC $\delta$  (+/+)] and PKC $\delta$  (-/-) mice after asbestos inhalation ( $\sim 7$  mg/m<sup>3</sup> air, 6 h/day, 5 d/week for 3, 9, or 40 d) was used to identify transcriptional changes in MMPs. Asbestos exposure resulted in significant increases in MMP12 mRNA levels in the lungs of WT mice at 3, 9, and 40 d (Fig 1A). Asbestos-induced up-regulation of MMP12 mRNA levels was significantly attenuated in PKC $\delta$  (-/-) mice (Fig 1B). Gene profiling also revealed an elevation of MMP13 levels after asbestos inhalation for 9 d that was reduced in PKC $\delta$  (-/-) mice (Fig 1C). Microarray results were confirmed and expanded using ribonuclease protection assays [rNase protection assay (RPA)] ( $n=6$  mice/group/time point). Increased steady-state mRNA levels of MMP12, MMP13, and TIMP1 were observed in lungs of WT mice exposed to asbestos, whereas other MMPs (MMP3, 7, 8, and 9) and TIMP2 and 3 did not change.

As observed in microarrays, PKC $\delta$  (-/-) mice showed reduced steady-state mRNA levels of MMP12 and MMP13 compared with WT animals. PKC $\delta$  (-/-) did not inhibit asbestos-induced TIMP1 mRNA levels.

#### 2. Asbestos increases steady-state mRNA levels of MMP12, MMP13, and TIMP1 in a time-dependent manner in lung epithelial cells and fibroblasts

In vitro studies were performed to determine the mechanisms of MMP up-regulation and relevant signaling pathways in epithelial cells and fibroblasts, the known target cell types of asbestos-induced lung cancers and fibrosis, respectively. Murine alveolar epithelial type II cells (C10) exposed to asbestos (5  $\mu$ g/cm<sup>2</sup>) for 4, 8, and 24 h showed time-dependent increases in steady-state mRNA levels of MMP13 and TIMP1 as determined by RPA. Primary lung fibroblasts also showed time-dependent increases in steady-state mRNA levels of MMP12, MMP13, and TIMP1 after exposure to asbestos. MMP12 was abundant in fibroblasts but was undetectable in epithelial cells as confirmed by quantitative reverse-transcriptase polymerase chain reaction (TaqMan).

To show that increased steady-state mRNA levels of MMPs by asbestos were not due to stabilization of mRNA, epithelial cells were treated with actinomycin D at different concentrations (50, 100, 200, 500 ng/ml) for 30 min prior to exposure to asbestos. Pretreatment with actinomycin D completely blocked asbestos-induced increases in MMP13 and TIMP1 mRNA, indicating transcriptional up-regulation of MMP13 and TIMP1 by asbestos.

<sup>1</sup>Correspondence: Department of Pharmacology, University of Vermont, 89, Beaumont Ave., Burlington, VT 05405, USA. E-mail: karen.lounsbury@uvm.edu  
doi: 10.1096/fj.05-4554fje

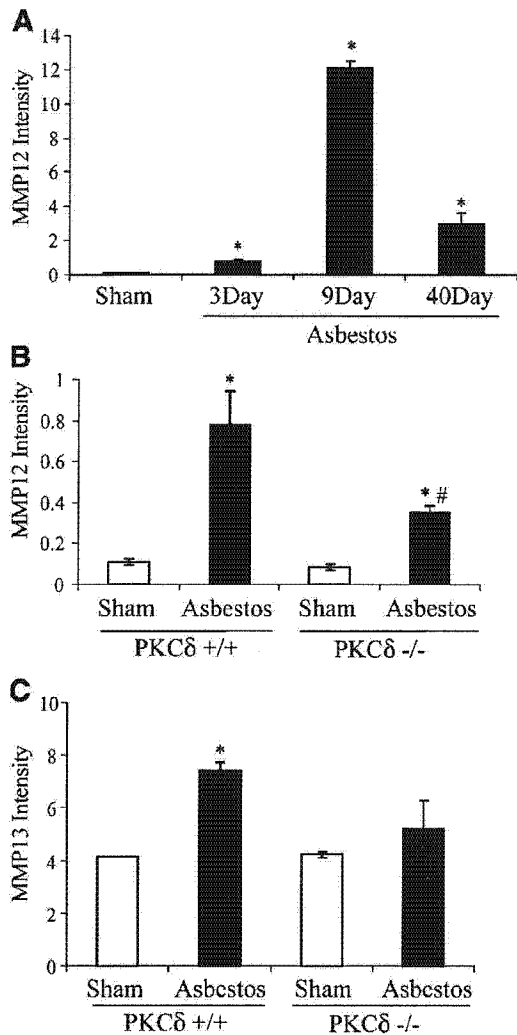


**Figure 1.** Asbestos inhalation causes increases in steady-state mRNA levels of lung MMP12, MMP13, and TIMP1 in WT mice [PKC $\delta$ (+/+)]]; MMP12 and MMP13 are inhibited in PKC $\delta$ (-/-) mice. WT and PKC $\delta$ (-/-) mice were exposed to asbestos (7 mg/m<sup>3</sup>, 6 h/day, 5 d/week for 3, 9, or 40 d). RNA was prepared from the lung, purified, and subjected to microarray analysis using an U74Av2 oligonucleotide chip. Data were analyzed using the GeneSifter program and validated by ribonuclease protection assays (RPAs). *A*) Time-dependent effects of asbestos inhalation on MMP12. *B*) Effect of asbestos inhalation (3 d) on MMP12 levels in PKC $\delta$ (-/-) mice. *C*) Effect of asbestos inhalation (9 d) on MMP13 levels in WT and PKC $\delta$ (-/-) mice. \* $P \leq 0.05$  compared with respective control group, # $P \leq 0.05$  as compared with asbestos exposed group.

### 3. Multiple cell signaling pathways are involved in regulation of asbestos-induced MMP12, MMP13, and TIMP1

To reveal the signaling pathways involved in regulation of MMPs and TIMP1 transcription by asbestos, C10 cells (MMP13 and TIMP1) or primary lung fibroblasts (MMP12) were exposed to different small molecule kinase inhibitors before addition of asbestos for 24 h.

As shown in **Fig 2A**, pretreatment of cells with an ERK1/2 inhibitor (U1026, 10  $\mu$ M) decreased asbestos-associated increases in MMP12, MMP13, and TIMP1. Whereas the PI3K inhibitor LY294002 (10 and 20  $\mu$ M) inhibited transcription of both MMP12 and MMP13 by asbestos, the EGFR phosphorylation inhibitor AG1478 (10 and 20  $\mu$ M) inhibited MMP13 expression significantly but MMP12 expression only slightly (**Fig 2B**). The PKC $\delta$ -specific inhibitor rottlerin (5  $\mu$ M) blocked asbestos-induced transcription of both MMP12 and MMP13; however, a general PKC inhibitor, bisindoly-

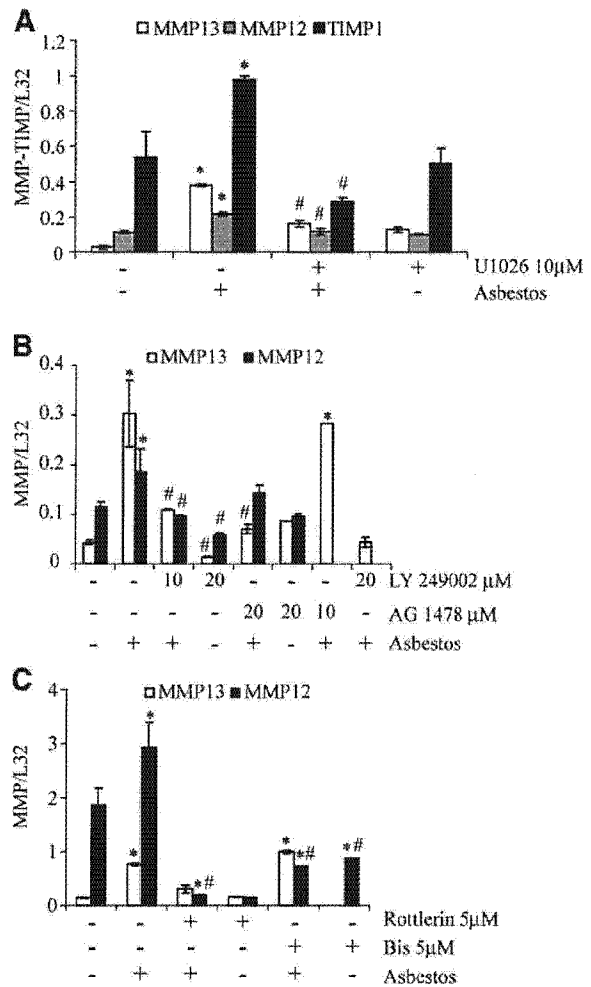


**Figure 2.** Asbestos-induced MMPs are regulated via an EGFR (or other growth factor receptors)/PI3K/PKC $\delta$ /ERK1/2 pathway. Lung epithelial type II cells (C10) (MMP13, TIMP1) and primary lung fibroblasts (MMP12) were pretreated with either *A*) a mitogen-activated protein kinase (ERK1/2) inhibitor (U1026 10  $\mu$ M for 1 h), *B*) a phosphatidylinositol 3-kinase (PI3K) inhibitor (LY 294002, 10 or 20  $\mu$ M for 1 h), or an EGF receptor inhibitor (AG1478, 10 or 20  $\mu$ M for 1 h) or *C*) a protein kinase C general inhibitor (Bis 5  $\mu$ M for 1 h) or PKC $\delta$  specific inhibitor (rottlerin 5  $\mu$ M for 1 h), before exposing them to asbestos (5  $\mu$ g/cm<sup>2</sup>) for 24 h. RNA was prepared and analyzed by a ribonuclease protection assay (RPA). Quantitation of autoradiograms was performed using a phosphorimager. \* $P \leq 0.05$  compared with untreated control, # $P \leq 0.05$  as compared to asbestos-exposed group.

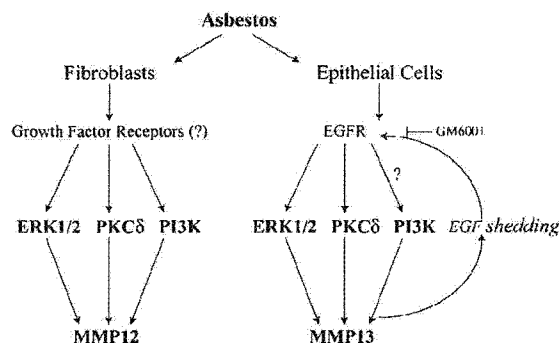


**Figure 3.** Hypothesis for the regulation of MMPs by asbestos. Asbestos exposure results in EGFR activation in epithelial cells and/or other growth factor receptors in fibroblasts, which leads to activation of PI3K/PKC $\delta$ /ERK1/2 and MMPs. MMPs once activated can further activate EGFR and downstream signaling pathways in epithelial cells. Inhibition of MMPs by GM6001 inhibited asbestos-induced ERK1/2 phosphorylation and EGFR activation in epithelial cells. EGF; EGFR, EGF receptor; ERK1/2, extracellular signal regulated kinase; GM6001, broad-spectrum MMP inhibitor; PI3K, phosphatidylinositol 3-kinase; PKC $\delta$ , protein kinase C delta.

maleimide I (Bis, 5  $\mu$ M), inhibited asbestos-induced up-regulation of MMP12 but had no effect on steady-state mRNA levels of MMP13 (Fig 2C).

#### 4. MMPs regulate asbestos-induced EGFR activation and ERK1/2 phosphorylation

To directly show the consequences of MMPs up-regulated by asbestos, C10 cells were pretreated with the broad range MMP inhibitor GM6001 (10  $\mu$ M), 1 h prior to addition of asbestos fibers for 8 h. GM6001 significantly inhibited both asbestos-induced ERK1/2 phosphorylation and EGFR activation. These events may be mediated by shedding of EGF by MMPs (a known phenomenon), which can then activate EGFR and downstream ERK1/2 signaling. These studies show that asbestos can up-regulate MMPs via multiple signaling pathways and that MMPs can further activate

asbestos-induced responses via subsequent activation of EGFR (Fig. 3) in epithelial cells.

#### CONCLUSIONS AND SIGNIFICANCE

Asbestos fibers cause pulmonary fibrosis and lung cancers, diseases that involve epithelial cell-fibroblast interactions and result in lung remodeling. MMPs are a family of secreted or transmembrane zinc-dependent endopeptidases that can degrade extracellular matrix (ECM) and basement membrane components and may be important in re-epithelization and remodeling of damaged lungs. In addition to enhancing ECM turnover and tissue remodeling, MMPs may also have profound effects on the release of pro-fibrotic growth factors and cytokines.

We show that asbestos exposure causes increased MMP12, MMP13, and TIMP1 transcription both in vitro (lung epithelial cells and fibroblasts) and after inhalation of fibers. Using PKC $\delta$  (-/-) mice, we also show that PKC $\delta$  plays an important role in transcriptional up-regulation of asbestos-induced MMP12 and MMP13. Further studies using cell cultures and small molecule inhibitors showed that asbestos-induced MMP up-regulation is dependent on signaling by growth factor receptors as well as the PI3K, PKC $\delta$  and ERK1/2 pathways.

MMPs up-regulated by asbestos can further activate asbestos-induced signaling pathways in epithelial cells. Inhibition of MMPs inhibited EGFR activation and ERK1/2 phosphorylation by asbestos, suggesting a role for MMPs in previously characterized asbestos-induced signaling pathways. In support of our findings several studies have shown that various MMPs play a critical role in shedding of EGF and activation of the EGFR.

In conclusion, our study is the first demonstration that asbestos can transcriptionally up-regulate MMP12 and MMP13 in a growth factor receptor/PI3K/PKC $\delta$ /ERK1/2-dependent manner (Fig. 3). Once up-regulated, MMPs can further activate asbestos-induced signaling pathways via EGFR activation. The interplay between asbestos-induced MMPs and TIMPs may be crucial in the development of asbestos-induced lung diseases, and relevant signaling pathways or MMPs may be targeted for intervention and therapy. FJ

## Transcriptional up-regulation of MMP12 and MMP13 by asbestos occurs via a PKC $\delta$ -dependent pathway in murine lung

Arti Shukla,\* Trisha F. Barrett,\* Keiichi I. Nakayama,<sup>†</sup> Kieko Nakayama,<sup>†</sup> Brooke T. Mossman,\* and Karen M. Lounsbury\*<sup>1</sup>

\*Departments of Pathology and Pharmacology, University of Vermont, USA, Burlington, Vermont, USA; and <sup>†</sup>Department of Molecular Genetics, Medical Institute of Bioregulation, Kyushu University, Fukuoka, Japan

**ABSTRACT** Asbestos is a known inflammatory, carcinogenic, and fibrotic agent, but the mechanisms leading to asbestos-induced lung diseases are unclear. Using a murine inhalation model of fibrogenesis, we show that asbestos causes significant increases in mRNA levels of lung matrix metalloproteinases (MMPs 12 and 13) and tissue inhibitor of metalloproteinases (TIMP1), as well as increased activities of MMP 2, 9, and 12 in bronchoalveolar lavage fluids (BALF). Asbestos-exposed PKC $\delta$  knockout (PKC $\delta$ -/-) mice exhibited decreased expression of lung MMP12 and MMP13 compared with asbestos-exposed wild-type mice. Studies using small molecule inhibitors in murine alveolar epithelial type II cells (C10) and primary lung fibroblasts confirmed that asbestos transcriptionally up-regulates MMPs via an EGFR (or other growth factor receptors)/PI3K/PKC $\delta$ /ERK1/2 pathway. Moreover, use of a broad-spectrum MMP inhibitor showed that MMPs play an important role in further enhancing asbestos-induced signaling events by activating EGFR. These data reveal a potentially important link between asbestos signaling and integrity of the extracellular matrix (ECM) that likely contributes to asbestos-induced lung remodeling and diseases.—Shukla, A., Barrett, T. F., Nakayama, K. I., Nakayama, K., Mossman, B. T., Lounsbury, K. M. Transcriptional up-regulation of MMP12 and 13 by asbestos occurs via a PKC $\delta$ -dependent pathway in murine lung. *FASEB J.* 20, E160–E169 (2006)

**Key Words:** TIMP • fibrosis • lung cancer • lung epithelium

THE DEVELOPMENT OF cancers (lung cancer, mesothelioma) and pulmonary fibrosis (asbestosis) is associated with the inhalation of asbestos fibers [reviewed in (1, 2)]. Although these diseases have been studied intensely by basic and clinical research scientists, little is known about the crucial cellular mechanisms that initiate and drive the processes of carcinogenesis and fibrogenesis. A multiplicity of interactions between effector cells of the immune system (alveolar macro-

phages, neutrophils, lymphocytes) and target cells, including bronchiolar and alveolar epithelial cells and fibroblasts, may govern the pathogenesis and progression of these diseases. We have shown previously that oxidative stress by asbestos fibers is linked causally to inflammation and the development of pulmonary fibrosis (3), as well as airway epithelial cell injury and proliferation (4).

Matrix metalloproteinases (MMPs) and tissue inhibitors of metalloproteinases (TIMPs) appear to be critical in the development and maintenance of lung architecture and function, their dysregulation resulting in lung damage, and remodeling (5–7). Abnormal ECM deposition is observed in the lungs of patients with idiopathic pulmonary fibrosis (IPF), due in part to an imbalance between MMPs and TIMPs (8, 9). Gene expression analysis also reveals that matrilysin (MMP7) may be a key regulator of pulmonary fibrosis in mice and humans (10).

In the pathogenesis of lung cancers and fibrosis, MMPs may be critical, not only in the breakdown and remodeling of lung tissues but also in the release and/or activation of profibrotic growth factors such as insulin growth factors (IGFs), transforming growth factor-beta (TGF- $\beta$ ), and tumor necrosis factor-alpha (TNF- $\alpha$ ) (11–13).

We have previously shown a role for PKC $\delta$  signaling in the regulation of proliferation and apoptosis of lung epithelial cells exposed to asbestos (14, 15). In the present investigation, using a mouse inhalation model of fibrogenesis (16) and isolated lung epithelial cells (C10 line) and fibroblasts, we show for the first time that asbestos causes up-regulation of MMPs 12 and 13 via a PKC $\delta$ -dependent pathway. In vitro studies also implicate interactions between phosphatidylinositol 3 kinase (PI3K)-PKC $\delta$ -extracellular signal-regulated kinase (ERK1/2) pathways in transcriptional up-regula-

<sup>1</sup>Correspondence: Department of Pharmacology, University of Vermont College of Medicine, 89 Beaumont Ave. Burlington, VT 05405, USA. E-mail: karen.lounsbury@uvm.edu

doi: 10.1096/fj.05-4554fje



tion of MMP12 and MMP13. Increases in expression of MMP12 and MMP13 in lung tissues of normal asbestos-exposed mice were attenuated in asbestos-exposed PKC $\delta$  knockout [PKC $\delta$  (-/-)] mice, confirming a regulatory role of PKC $\delta$  in MMP transcription. Finally, we show that MMPs up-regulated by asbestos stimulate asbestos-induced signaling pathways via activation of the EGFR in epithelial cells.

## MATERIALS AND METHODS

### Inhalation experiments

Animal experiments were conducted in accordance with the NIH Guide for the Care and Use of Laboratory Animals (publication 85-23, 1985) following protocols approved by the University of Vermont Institutional Animal Care and Use Committee. C57Bl/6 mice (8 to 12 wk of age) were exposed to ambient air or the NIEHS reference sample of chrysotile asbestos (7 mg/m<sup>3</sup> air; 6 h/day; 5 d/week for 3, 9, or 40 d) as described previously (16). Briefly, mice were euthanized with an intraperitoneal (i.p.) injection of pentobarbital (Abbott Laboratories, Abbot Park, IL), chest cavities were opened, and lungs were cannulated via the trachea with polyethylene tubing. Lungs were then lavaged 1 $\times$  with sterile Ca<sup>2+</sup>- and Mg<sup>2+</sup>-free PBS at a vol of 1 ml. The vol of retrieved PBS in bronchoalveolar lavage fluid (BALF) was also recorded. One lung lobe was excised following lavage and stored in RNAlater (Ambion, Austin, TX) for RNA analysis using ribonuclease protection assays rNase protection assay (RPA) and Affymetrix microarray analyses (Affymetrix Inc., Santa Clara, CA). BALF was centrifuged at 600 *g* to obtain a cell-free supernatant for MMP activity assays using gelatin zymography (see below).

### PKC $\delta$ (-/-) mice

A breeding pair of PKC $\delta$  ( $\pm$ ) mice (17), originally bred into the C57Bl/6 background, was a kind gift from Dr. K. I. Nakayama. These mice were subsequently maintained in the UVM facility and bred into the C57Bl/6 background 4-6 $\times$  before use with normal wildtype (WT) [PKC $\delta$  (+/+)] littermates in inhalation experiments. Tail DNA was evaluated using the polymerase chain reaction (PCR), and primers for PKC $\delta$  were obtained from MWG Biotech, Inc. (High Point, NC). Lung tissue from PKC $\delta$  (-/-) mice was examined by Western blot analyses using antibodies for PKC $\delta$  and other isoforms ( $\alpha$ ,  $\zeta$ ,  $\theta$ ) of PKC (Santa Cruz Biotechnology, Inc., Santa Cruz, CA) to confirm that only PKC $\delta$  protein is absent while other isoforms of PKC are present.

### Cell cultures and exposures to agents

A contact inhibited, nontransformed murine alveolar epithelial type II cell line (C10) (18) was propagated in CMRL-1066 medium containing penicillin (100 U/ml), streptomycin (100  $\mu$ g/ml), L-glutamine (2 mM), and 10% FBS (Life Technologies, Inc., Grand Island, NY). For all experiments, cells were grown to confluence, complete medium was removed, and medium containing 0.5% FBS or no serum was added 24 h before exposure to agents. Primary mouse lung fibroblasts were isolated from 10-wk-old C57Bl/6 mice using an enzyme digestion method (collagenase-trypsin-DNase) and propagated in Dulbecco's modified Eagle medium (DMEM, GIBCO Life Technologies, Inc., Grand Island, NY)

with 10% FBS, penicillin, streptomycin, and L-glutamine at concentrations above. Antibodies for phosphorylated form (p-ERK44/42) and total ERK1/2 (ERK44/42) and EGFR were from Cell Signaling (Beverly, MA). Inhibitors of PI3K (LY249002, 10 and 20  $\mu$ M), ERK1/2 (U1026, 10  $\mu$ M), PKC $\delta$  [Rottlerin, 5  $\mu$ M (19)], general PKCs (Bisindolymaleimide I, 5  $\mu$ M), EGFR phosphorylation (AG1478, 10 and 20  $\mu$ M) and broad-spectrum MMP inhibitor (GM6001, 10  $\mu$ M) were obtained from Calbiochem (La Jolla, CA) and used at nontoxic and selective concentrations in vitro as reported previously (15, 20-23). These inhibitors were added 1 h prior to addition of asbestos. Actinomycin D (inhibitor for RNA synthesis, 50-500 ng/ml), gelatin, and Briz 35 were purchased from Sigma Chemical Co. (St. Louis, MO). Standard gelatinase mix was obtained from Chemicon International (Chemicon International, Temecula, CA).

For in vitro studies, crocidolite asbestos fibers (Na<sub>2</sub>(Fe<sup>3+</sup>)<sub>2</sub>(Fe<sup>2+</sup>)<sub>8</sub>(OH)<sub>2</sub>[Si<sub>8</sub>O<sub>22</sub>]) (NIEHS reference sample) were suspended in Hank's balanced salt solution (HBSS) (Life Technologies, Inc. Grand Island, NY) at 1 mg/ml, sonicated, and then triturated 10 $\times$  through a 22-gauge needle to obtain a homogenous suspension before addition directly to medium at noncytolytic concentrations of 5  $\mu$ g/cm<sup>2</sup> surface area of culture dish. Because available samples of NIEHS reference samples of crocidolite are limited and insufficient in quantities required for inhalation experiments, NIEHS reference standards of chrysotile asbestos (Mg<sub>3</sub>[Si<sub>2</sub>O<sub>5</sub>](OH)<sub>4</sub>) were used in animal studies. Long fibers ( $\geq 5$   $\mu$ m) of both crocidolite and chrysotile asbestos are fibrogenic and carcinogenic and cause oxidant generation from cells via frustrated phagocytosis or iron catalyzed reactions (i.e., crocidolite) (4). NIEHS crocidolite and chrysotile reference samples of asbestos have been characterized previously for their chemical and physical properties (24).

### Microarray analysis for MMP mRNA levels in lungs

Total RNA was isolated from lung tissues as described above using TriZol reagent (Invitrogen, Life Technologies, CA) and submitted to the Vermont Cancer Center Microarray Facility for target preparation using standard Affymetrix protocols. Briefly, 3  $\mu$ g of total RNA from each sample was reverse-transcribed using oligo-dT primer coupled to a T7 RNA polymerase binding sequence. Following double-stranded cDNA preparation, biotinylated-cRNA was synthesized using T7 polymerase and hybridized to Affymetrix murine genome U74Av2 oligonucleotide arrays for 16 h. The arrays were first incubated with a streptavidin-conjugated to phycoerythrin, followed by sequential incubation with biotin-coupled polyclonal antistreptavidin antibody (Ab) and streptavidin-phycoerythrin as an amplification step. After washing and laser scanning (Hewlett-Packard GeneArray Scanner, Agilent Technologies, Inc.), data were collected and analyzed by using GeneSifter software (GeneSifter VizX Labs, Seattle, WA). Results were confirmed by RPA using a larger number of animals per group ( $n=6$ ).

### Ribonuclease protection assays (RPA)

Total RNA was prepared from cells and murine lung tissue after 9 and 40 d of exposure to asbestos as described by Shukla et al. (25). Steady-state mRNA levels of MMP3, MMP7, MMP8, MMP9, MMP12, MMP13, TIMP1, TIMP2, TIMP3, and the ribosomal probe L32 and glyceraldehyde-3-phosphate dehydrogenase (GAPDH) were examined with a RiboQuant multiprobe RPA system and the mMMP2 multiprobe template set (Pharmingen, San Diego, CA) according to the manufacturer's protocol. Autoradiograms were quantitated

with a Bio-Rad (Richmond, CA) phosphoimager. Results were normalized to expression of the housekeeping gene, L32.

#### TaqMan [Quantitative reverse transcriptase PCR (RT-PCR)]

Total RNA was extracted from cells as described for the RPA and then further purified using an RNA cleaning kit (Qiagen Inc., Valencia, CA) according to the manufacturer's instructions. Samples were also treated with RNase-free DNase I to remove contaminating genomic DNA. The RNA was then used to generate cDNA with the Reverse Transcription System (Promega, Madison, WI), according to the manufacturer's instruction. The Perkin-Elmer ABI 7700 prism Sequence Detection System (Applied Biosystems, Foster City, CA) was used to determine relative levels of expression of MMP12. All values were normalized to the expression of HPRT (TaqMan primers and probes for MMP12 and HPRT were purchased from Applied Biosystems).

#### Zymography on BALF samples from mice

BALF from sham and asbestos-exposed mice after 9 or 40 d of asbestos inhalation was collected for determination of MMP activity. The BALF was centrifuged at 600 X g for 5 min, and the supernatant was recovered and frozen at  $-70^{\circ}\text{C}$ . Cell-free BALF (75  $\mu\text{l}$ ) was subjected to SDS-PAGE under nonreducing conditions. MMP activity was determined by in gel zymography with gelatin (Type A from Porcine skin, Sigma) as a substrate. Samples were loaded under nonreducing conditions onto 4% stacking/10% separating SDS-polyacrylamide gels with 1 mg/ml gelatin polymerized in the separating gel before electrophoresis. After separation, gels were washed 3X in 2.5% Triton X-100 for 20 min with gentle shaking. All gels were incubated for 48 h at  $37^{\circ}\text{C}$  in substrate buffer (50 mM Tris.HCl, pH 7.6, 5 mM  $\text{CaCl}_2$ , 0.05% Brij 35, and 0.02%  $\text{NaN}_3$ ), stained in Coomassie blue R-250 in 7% acetic acid and 40% methanol, and then destained in 7% acetic acid and 40% methanol. Clear, digested regions represented MMP activity and were identified based on MW markers (MMP12) as described by Shipley et al. (26) and/or standard gelatinases (MMP 2 and 9, Chemicon Int., CA). MMP identity was confirmed by an additional 30 min incubation of selected gels with the metal chelators EDTA (10 mM).

#### Western blot analysis for extracellular signal-regulated kinases (ERK1/2 and p-ERK1/2)

Cells grown in culture dishes were washed three times with ice-cold PBS and collected in lysis buffer (20 mM Tris, pH 7.6; 1% Triton-X100; 137 mM NaCl; 2 mM EDTA; 1 mM  $\text{Na}_2\text{VO}_4$ ; 1 mM DTT; 1 mM phenylmethylsulfonyl fluoride; 10  $\mu\text{g}/\text{ml}$  leupeptin; and 10  $\mu\text{g}/\text{ml}$  aprotinin) before incubation on ice for 30 min. Cells were then sonicated (3 bursts of 5 s each) and centrifuged at 14,000 rpm for 15 min at  $4^{\circ}\text{C}$ . Supernatants were collected, and protein concentrations were determined using the Bradford assay (Bio-Rad). Cell lysates (40  $\mu\text{g}$ ) were resolved by SDS-PAGE and transferred to nitrocellulose membranes according to standard procedures. Equal loading of protein was verified by Ponceau stain (Sigma). Membranes were washed in TBS, blocked for 30 min with TBS containing 5% nonfat milk, then incubated with primary antibodies at 1:1000 (p-ERK1/2, ERK1/2) dilution in TBS containing 1% BSA (0.01% Azide) overnight at  $4^{\circ}\text{C}$ . Membranes were then washed twice with TBS alone and twice with PBS containing 0.1% Tween 20 before incubation with horseradish peroxidase-conjugated secondary Ab (1:5000 in PBS containing 0.1% Tween 20 and 5% nonfat milk) for 1 h at room temperature. Membranes were washed once with PBS

containing 0.1% Tween 20 and 3 times with PBS before Ab binding was visualized by enhanced chemiluminescence (Amersham Pharmacia Biotech, Piscataway, NJ) according to the manufacturer's protocol.

#### Kinase activity assay for epidermal growth factor receptor (EGFR)

EGFR kinase activity was determined with an immunoprecipitation kinase assay as follows. Soluble protein was prepared as described elsewhere (15); the protein (300  $\mu\text{g}$ ) then was immunoprecipitated for 2 h at  $4^{\circ}\text{C}$  with an anti-EGFR Ab (1:100, Cell Signaling); and the antigen-antibody complexes were collected by incubation with agarose protein A (Life Technologies, Inc.) for 1 h at  $4^{\circ}\text{C}$ . Then, pellets were washed three times with lysis buffer and three times with kinase buffer (20 mM HEPES, pH 7.4; 10 mM  $\text{MnCl}_2$ ; 10 mM  $\text{MgCl}_2$ ; 1 mM DTT; 100  $\mu\text{M}$   $\text{Na}_2\text{VO}_4$ ; and 10  $\mu\text{M}$  ATP) before resuspension in a reaction buffer containing 25  $\mu\text{l}$  kinase buffer, myelin basic protein (MBP, 5  $\mu\text{g}$ ), and 5  $\mu\text{Ci}$  of  $[\gamma\text{-}^{32}\text{P}]\text{ATP}$  (New England Nuclear, Life Science Products, Inc., Boston, MA). All of the samples were incubated for 20 min at  $30^{\circ}\text{C}$ . Reactions were terminated by addition of 2X SDS sample buffer and boiled, and the reaction products were resolved on a 15% SDS-polyacrylamide gel. The extent of myelin basic protein phosphorylation was determined by autoradiography.

*Statistical analyses* In all experiments, duplicate or triplicate determinations per group per time point were performed. Experiments were repeated 3X or more. Results were evaluated by one-way ANOVA with the Student-Newman-Keuls procedure for adjustment of multiple pair-wise comparisons between treatment groups. Differences of  $P \leq 0.05$  were considered statistically significant.

## RESULTS

### Asbestos inhalation causes up-regulation of MMP12, MMP13, and TIMP1 mRNA levels in lung: MMP12 and MMP13 are inhibited in PKC $\delta$ (-/-) mice

#### Microarray analysis of lung tissue

Oligonucleotide microarray analysis (Affymetrix) on RNA prepared from whole lungs of mice ( $n=3/\text{group}$ ) was used to verify transcriptional changes in MMPs in asbestos-exposed lungs. As shown in Fig. 1A, asbestos exposure resulted in significant increases in MMP12 mRNA levels in the lungs of WT mice at 3, 9, and 40 d. Significant attenuation of asbestos-induced up-regulation of MMP12 mRNA levels occurred in PKC $\delta$  (-/-) mice (Fig. 1B, (3 d)). Gene profiling also revealed an elevation of MMP13 levels after asbestos inhalation for 9 d that was reduced in PKC $\delta$  knockout mice (Fig. 1C). The complete results of microarray analyses of sham and asbestos-exposed WT mice have been recently published (27).

#### Ribonuclease protection assays

The microarray data were confirmed by ribonuclease protection assays using a larger number of animals. After 9 or 40 d of asbestos inhalation, lungs from WT and PKC $\delta$  (-/-) mice ( $n=6/\text{group}/\text{time period}$ ) were

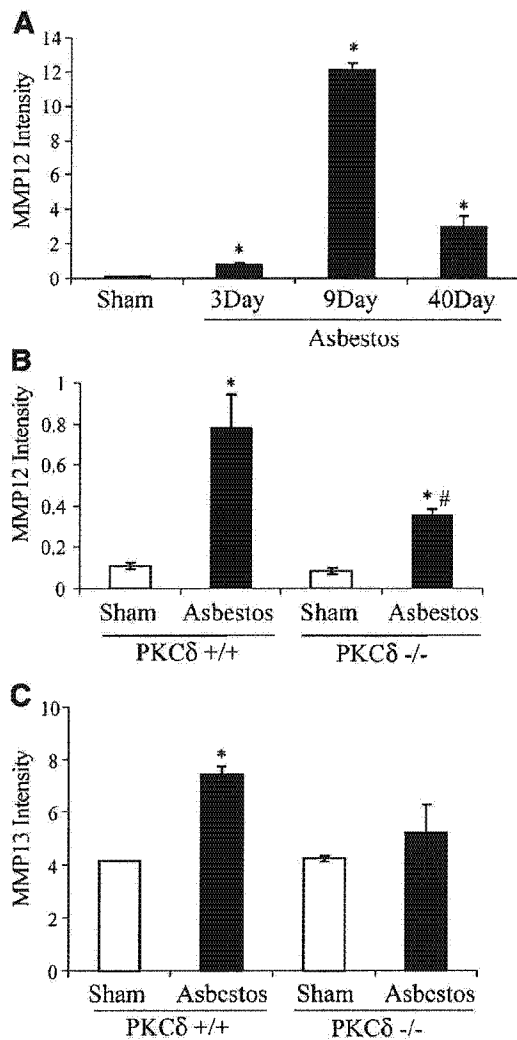


**Figure 1.** Microarray analysis showing that asbestos inhalation causes increases in lung mRNA levels of MMP12 and 13, which are inhibited in PKC $\delta$  (-/-) mice. PKC $\delta$  (-/-) mice and WT littermates bred into the C57Bl/6 background were exposed to asbestos (7 mg/m<sup>3</sup>, 6 h/day, 5 d/wk) for 3, 9, or 40 d. RNA was prepared from the lung, purified, and subjected to microarray analysis using an U74Av2 oligonucleotide chip. Data were analyzed using the GeneSifter program. A) Time-dependent effects of asbestos inhalation on MMP12. B) Effect of asbestos inhalation (3 d) on MMP12 levels in PKC $\delta$  (-/-) mice. C) Effect of asbestos inhalation (9 d) on MMP13 levels in WT and PKC $\delta$  (-/-) mice. \* $P \leq 0.05$  as compared with respective control group, # $P \leq 0.05$  compared with asbestos-exposed group. ( $n=3$  per group).

analyzed for steady-state mRNA levels of MMPs and TIMPs by ribonuclease protection assays. Increased levels of MMP12, MMP13, and TIMP1 were observed in lungs of WT mice exposed to asbestos for 9 d (Fig. 2A) and MMP12 levels remained elevated up to 40 d of asbestos exposure (data not shown), whereas levels of MMP3, 7, 8, 9, and TIMP2, 3 were similar to those of sham mice. As shown in Fig 2A, (a representative RPA showing two animals/group), PKC $\delta$  (-/-) mice showed attenuation of asbestos-induced steady-state mRNA lev-

els of MMP12 and MMP13 as compared to WT animals. Fig. 2B and C represents the quantitation of 9 d autoradiograms for MMP12 and MMP13, respectively, with each group having 6 animals.

#### MMP activity in BALF from WT and PKC $\delta$ (-/-) mice

BALF was analyzed for MMP activity using gelatin zymography. As shown in Fig. 3A, proMMP9, proMMP2 (identified based on standard gelatinases) and MMP12 activities [as identified based on MW (fully processed 22 kDa) as described by Shipley et al. (26)] were increased in BALF from 9 d asbestos-exposed animals. After 40 d of asbestos inhalation, MMP2 and MMP9 activity levels returned to normal control levels; however, MMP12 activity remained elevated in BALF (Fig. 3B). Gelatin zymography on BALF from both WT (Fig. 3A) and PKC $\delta$  (-/-) asbestos-exposed mice showed increased MMP2, MMP9, and MMP12 activities (Fig. 3C). The discrepancy between lack of inhibition in MMP12 activity vs. decreased MMP12 transcript levels in PKC $\delta$  (-/-) mice might be attributed to the altered inflammatory response shown by these animals in response to asbestos (28). High levels of MMP12 activity observed in PKC $\delta$  (-/-) sham animals could possibly be related to inflammatory patches we see in the lungs of these mice.

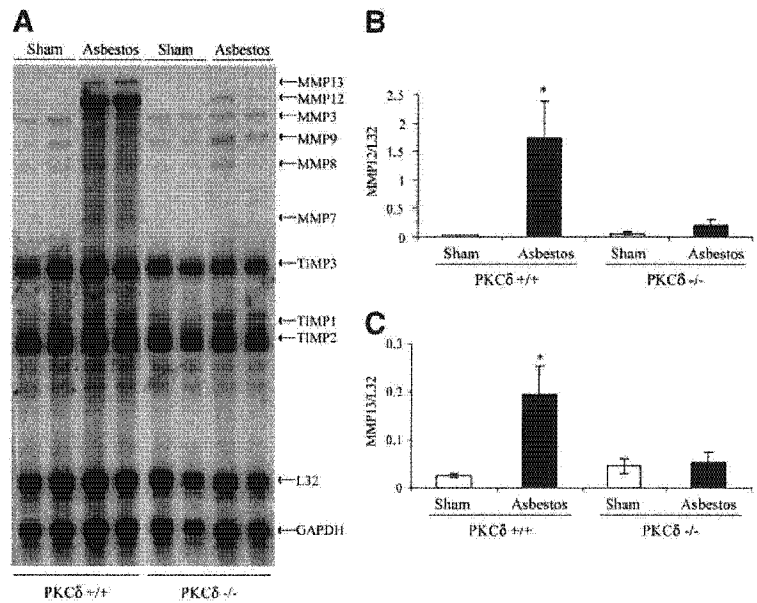
#### Asbestos increases steady-state mRNA levels of MMP12, MMP13, and TIMP1 in a time-dependent manner in lung epithelial cells and fibroblasts

In vitro studies were performed to determine the mechanisms of MMP up-regulation and relevant signaling pathways in lung epithelial cells and fibroblasts, target cell types of asbestos-induced lung cancers, and fibrosis, respectively. Exposure of C10 epithelial cells to asbestos (5  $\mu\text{g}/\text{cm}^2$ ) for 4, 8, and 24 h caused time-dependent increases in steady-state mRNA levels of MMP13 and TIMP1 as determined by RPA (Fig. 4A, B). Primary lung fibroblasts also showed time-dependent increases in steady-state mRNA levels of MMP12, MMP13, and TIMP1 after exposure to asbestos. MMP12 was abundant in fibroblasts but was undetectable in epithelial cells. The induction of MMP12 by asbestos in fibroblasts as detected by RPA was confirmed using quantitative RT-PCR (TaqMan) (Fig. 4C).

#### Asbestos affects transcription of MMP13 and TIMP1 in lung epithelial cells

To show that increased steady-state mRNA levels of MMP13 and TIMP1 by asbestos were not due to stabilization of mRNA, C10 cells were treated with actinomycin D (a transcription inhibitor) at different concentrations (50, 100, 200, 500 ng/ml) for 30 min prior to exposure to asbestos. Pretreatment with actinomycin D completely blocked asbestos-induced increases in MMP13 and TIMP1 mRNA (Fig. 5) as determined by

**Figure 2.** Asbestos inhalation causes increases in steady-state mRNA levels of lung MMP12, 13, and TIMP1 in wild-type mice; MMP12 and 13 are inhibited in PKC $\delta$  (-/-) mice. C57Bl/6 and PKC $\delta$  (-/-) mice ( $n=6$  per group) were exposed to chrysotile asbestos (7 mg/m<sup>3</sup>, 6 h/day, 5 d/wk) for 9 d. Lung RNA was prepared and analyzed by ribonuclease protection assay using an mMMP2 template. **A**) A representative autoradiogram using 2 mice per group (out of 24 mice run on the same gel). Quantitation of autoradiograms using 6 mice per group for MMP12 (**B**) and for MMP13 (**C**). \* $P \leq 0.05$  compared with untreated control.



RPA, indicating transcriptional up-regulation of MMP13 and TIMP1 by asbestos.

#### Multiple cell signaling pathways are involved in regulation of asbestos-induced MMPs

Asbestos exerts its effects on lung epithelial cell proliferation via EGFR dependent and independent pathways leading to ERK1/2 and ERK5 activation and activating protein (AP)-1 transactivation (29). To reveal the signaling pathways involved in regulation of MMP and TIMP transcription by asbestos, C10 epithelial cells (MMP13 and TIMP1) or fibroblasts (MMP12) were exposed to different small molecule kinase inhibitors before addition of asbestos for 24 h and then analyzed by RPA. As shown in Fig. 6A, pretreatment of cells with an ERK1/2 inhibitor (U1026, 10  $\mu$ M) decreased asbestos-associated increases in MMP12, MMP13, and TIMP1 mRNA. Whereas the PI3K inhibitor (LY294002 at 10 and 20  $\mu$ M) inhibited both MMP12 and MMP13 transcription by asbestos, the EGFR phosphorylation inhibitor (AG1478 10 and 20  $\mu$ M) inhibited MMP13 but not MMP12 mRNA expression by asbestos (Fig. 6B). The PKC $\delta$ -specific inhibitor rottlerin at 5  $\mu$ M blocked asbestos-induced transcription of both MMP12 and MMP13; however, a general PKC inhibitor (Bis at 5  $\mu$ M) inhibited asbestos-induced up-regulation of MMP12 but had no effect on steady-state mRNA levels of MMP13 (Fig. 6C), indicating different pathways of regulation in different cell types. Constitutive levels of MMP12 mRNA were also inhibited by rottlerin and Bis.

#### Asbestos-induced up-regulation of MMPs can further enhance signaling pathways via EGFR activation

Using a broad-spectrum inhibitor of MMPs (GM6001, 10  $\mu$ M), we show that inhibition of MMPs inhibits

asbestos-induced EGFR activation (Fig. 7A) and ERK1/2 phosphorylation (Fig. 7B, C) in C10 lung epithelial cells, indicating an important role of MMPs in initiation of asbestos-induced cell signaling. Addition of GM6001 alone to cells had no effects on EGFR or ERK1/2 phosphorylation.

## DISCUSSION

Asbestos fibers cause pulmonary fibrosis and lung cancers (2), diseases involving epithelial cell-fibroblast interactions and resulting in lung remodeling. MMPs are a family of secreted or transmembrane zinc-dependent endopeptidases that can degrade ECM and basement membrane components and may be important in re-epithelization and remodeling of damaged lungs. In addition to enhancing ECM turnover and tissue remodeling, MMPs may also have profound effects on the release of pro-fibrotic growth factors and cytokines (11–13).

Recent data implicate MMP7 or matrilysin as a key regulator of pulmonary fibrosis in mice and humans, and matrilysin knockout mice are resistant to pulmonary fibrosis (10). Histological examination of normal lungs and lungs from patients with interstitial lung disease also implicate changes in distribution and amounts of MMPs and TIMPs (30). Isolated alveolar macrophages obtained from untreated patients with idiopathic pulmonary fibrosis show marked increases in MMP9 secretion compared with macrophages collected from normal individuals (31). In addition, a synthetic inhibitor of MMP, Batimastat, reduces bleomycin-induced lung fibrosis (32). In studies here, we show that exposure to asbestos cause significant increases in MMP12, MMP13, and TIMP1 expression levels, which are attenuated in lungs of PKC $\delta$  (-/-) mice. These

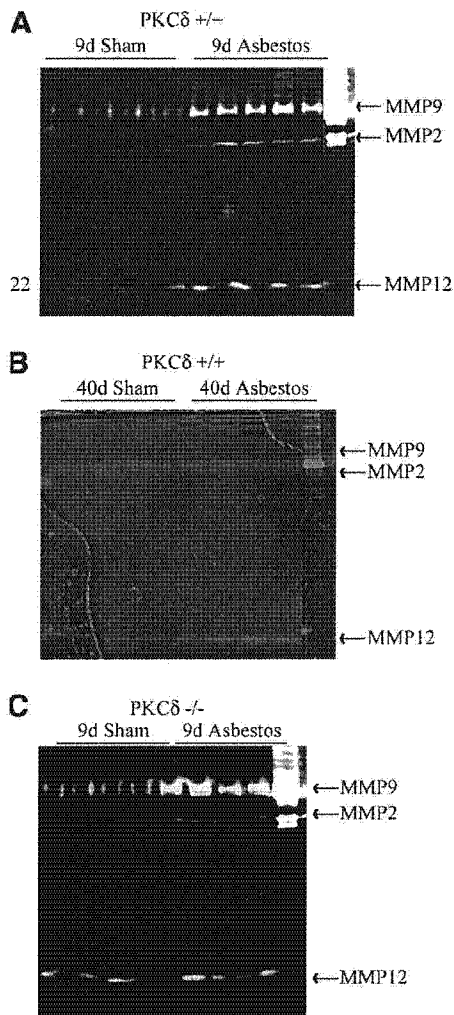


**Figure 3.** Gelatin zymogram showing increased MMP2, 9, and 12 activities in BALF after asbestos inhalation. PKC $\delta$  (-/-) mice and WT littermates were exposed to asbestos (7 mg/m<sup>3</sup>, 6 h/day, 5 d/wk) for 9 (A) or 40 (B). BAL fluid was collected, and gelatin zymography was run under nonreducing conditions. Clear digested areas were identified based on molecular wt markers (MMP12) and positive controls (MMP2 and 9). C) Zymogram from BALF of PKC $\delta$  (-/-) mice after 9 d of asbestos exposure.

changes may be explained by our observations that PKC $\delta$  (-/-) mice exhibit altered inflammatory profiles and less pulmonary fibrosis in response to asbestos in comparison to WT littermates (28). The observed increase in MMP12 activity in PKC $\delta$  (-/-) sham mice as compared to WT sham animals is hard to explain but might be related to altered immune responses and the presence of patches of inflammatory cells in lungs of PKC $\delta$  (-/-) mice.

Our results suggest that asbestos can induce ECM remodeling affecting both matrix deposition and degradation. For example, MMP13 (collagenase 3) is an epithelial matrix metalloproteinase that degrades mainly fibrillar collagens and gelatinases A and B (MMP2 and MMP9), which degrade type IV basement

membrane collagen (33). TIMP1 is a multifunctional molecule that inhibits matrix metalloproteinase activity and promotes the proliferation of receptive cells. Increased activity of MMP13 in BALF was not observed despite several-fold increases in mRNA levels of MMP13 in lung. This observation may reflect increased TIMP1 levels in lung that inhibited MMP13 activity. Increased expression of MMP13 and TIMP1 was also reported by Ortiz et al. (34) in a murine model of silicosis.

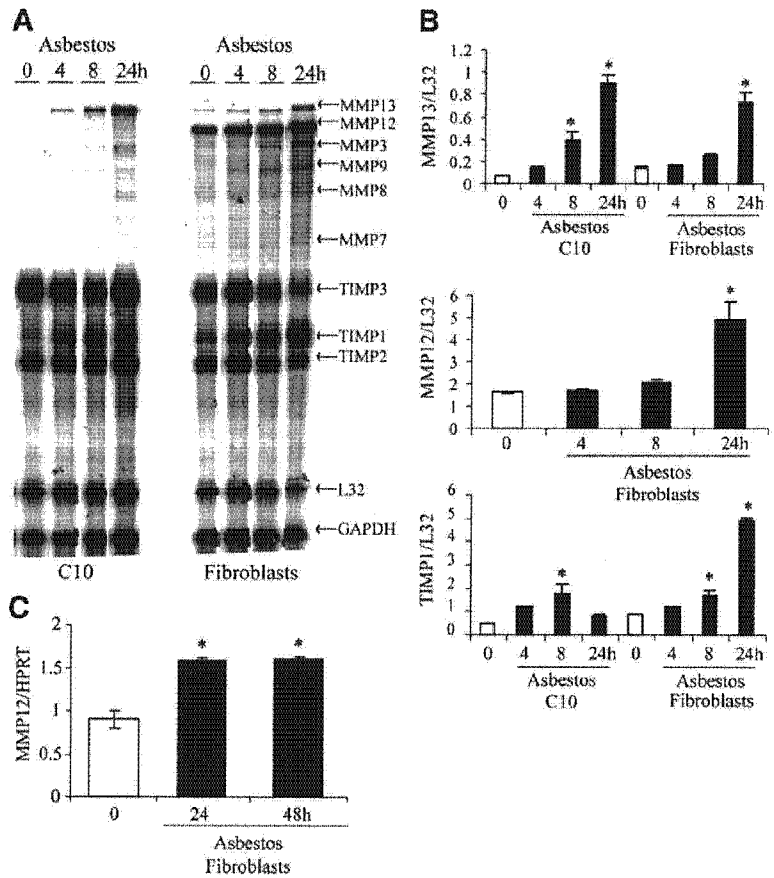
Here we show that inhalation of asbestos causes increases in mRNA levels and activity of MMP12. Macrophage metalloelastase (MME) or MMP12 can hydrolyze a broad spectrum of substrates (35, 36). Although most of the available literature indicates that the macrophage is the main cell type making MMP12, here we show for the first time that primary lung fibroblasts also express MMP12. MMP12 expression in this cell type was confirmed by two different techniques, RPA and quantitative RT-PCR (TaqMan), which revealed similar results (Fig. 4). In support of our observation that cells other than macrophages can also express MMP12, a recent report shows the induction of MMP12 gene expression in airway-like epithelial cell by cigarette smoke (37). Use of MMP12 knockout mice in our inhalation model may shed light on the importance of this protein in development of asbestos-induced fibrosis.

Asbestos inhalation also results in increased MMP2 and MMP9 activities in BALF, although no effect on transcript levels of these two MMPs was observed. These increases in activity could reflect contributions of increased inflammatory cells in BALF, which are features of this animal model (16).

MMP production and activity are highly regulated at different levels. In general, basal transcription in normal adult tissues is low, but MMPs are up-regulated by a variety of factors at the transcriptional, postranscriptional, and postranslational levels as well as by the interaction of secreted enzymes with TIMPs (7, 38). Our studies using epithelial cells and fibroblasts with small molecule inhibitors show that asbestos-induced increases in MMP12, MMP13, and TIMP1 mRNA levels are ERK1/2 dependent. These results are consistent with many studies showing that MMPs (MMP1, MMP3, MMP7, MMP9, MMP10, MMP12, and MMP13) are regulated by extracellular stimuli, which activate activator protein-1 (AP-1) [reviewed in (39, 40)]. Previous work from our laboratory has shown that asbestos activates AP-1 dependent gene transcription via the ERK1/2 pathway, whereas c-Jun NH2-terminal kinase and p38 pathways are not activated by asbestos (41). Experiments here reveal that asbestos-induced MMP12 and MMP13 expression are also regulated by EGF receptor (EGFR), phosphatidylinositol 3-kinase (PI3K), and PKC $\delta$ , results consistent with other reports implicating these pathways in MMP regulation by other agents (42, 43). For example, EGFR-mediated signaling promotes MMP9 activation by enhancing PI3K-dependent cell surface association of the receptor (44). Our studies indicate nonsignificant effects of an EGFR in-



**Figure 4.** Asbestos exposure causes time-dependent increases in MMPs and TIMP steady-state mRNA levels in lung epithelial cells and fibroblasts. Lung epithelial type II cells (C10) or primary lung fibroblasts were exposed to asbestos ( $5 \mu\text{g}/\text{cm}^2$ ) for different time periods (4 to 24 h). RNA was prepared and analyzed by ribonuclease protection assay using a mMMP2 template. Autoradiograms were developed (A) and selected genes were quantitated using phosphoimaging (B). Results are represented as a ratio to the housekeeping gene, L32.  $*P \leq 0.05$  in comparison to respective untreated control. C) Fibroblasts were exposed to asbestos for 24 or 48 h. RNA was prepared and analyzed by quantitative real-time PCR (TaqMan) for MMP12 levels.  $*P \leq 0.05$  in comparison to untreated controls.



inhibitor on asbestos-induced MMP12 mRNA levels in fibroblasts; however, asbestos-induced MMP13 mRNA levels in epithelial cells were significantly inhibited by higher concentrations (20  $\mu\text{M}$ ) of an EGFR inhibitor (Fig. 6B). These findings indicate that asbestos-induced

responses in epithelial cells occur via EGFR activation, whereas in fibroblasts other growth factor(s) may be responsible.

The MMPs play a critical role in the processing of EGF and EGF-like ligand precursors, thereby contributing to the EGFR signal transactivation (45–47). In our study, blocking of MMP activation with a broad-spectrum small molecule inhibitor GM6001 in epithelial cells inhibited asbestos-induced EGFR activation and ERK1/2 phosphorylation, an EGFR-dependent event in cells after exposure to asbestos or cigarette smoke (23, 48). This finding demonstrates that once MMPs are activated, they can further enhance asbestos-induced signaling pathways via EGFR activation.

We note that the results in our study have focused largely on the expression of MMP and TIMP transcripts, which may or may not always equate with protein expression. Although it is desirable to determine protein expression of MMPs or TIMPs as well, the reagents (e.g., antibodies) to detect most nongelatinase MMPs in mice, including MMP12 and MMP13, are rudimentary and the specificity suspect. Future studies to better define MMP protein expression and secretion will extend our current data.

Putting the current findings in the context of previous findings by our research group and others (49–51), we propose a new hypothetical model wherein asbestos transcriptionally up-regulates MMP12 and MMP13 in a

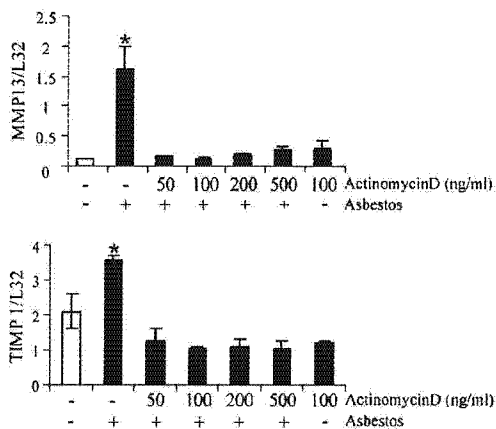


**Figure 5.** Asbestos transcriptionally up-regulates MMP13 and TIMP1. Lung epithelial type II cells (C10) were pretreated with various concentrations of actinomycin D (50–500 ng/ml) for 30 min before exposing them to asbestos ( $5 \mu\text{g}/\text{cm}^2$ ) for 24 h. RNA was prepared and analyzed by ribonuclease protection assays using a mMMP2 template. Quantitation of autoradiograms was performed using a phosphoimager.  $*P \leq 0.05$  as compared to untreated control.

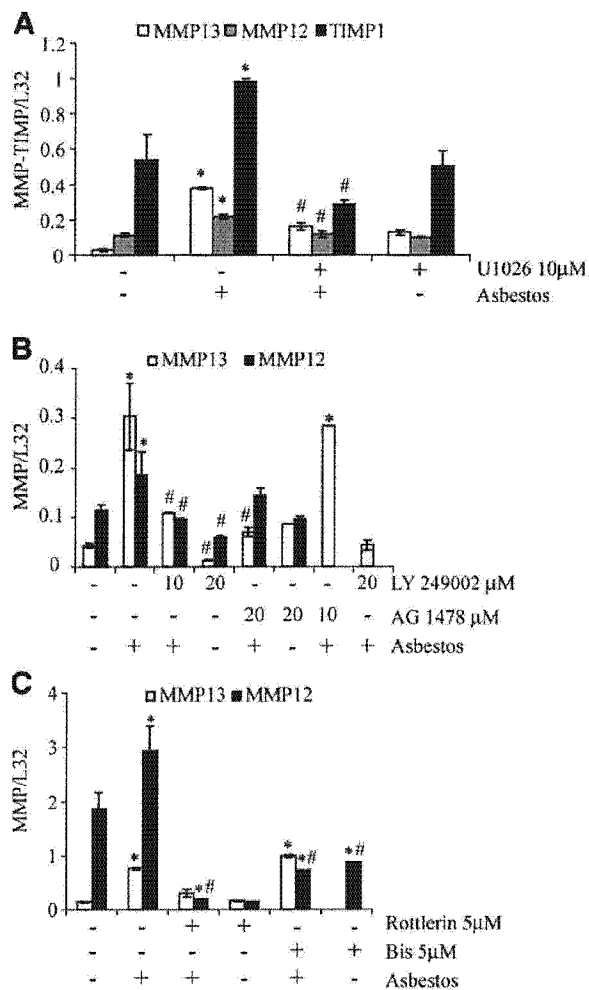


**Figure 6.** Asbestos-induced MMP12 and 13 are regulated via an EGFR (or other growth factor)/PI3K/PKCδ/ERK1/2 pathway. Lung epithelial type II cells (C10) and primary lung fibroblasts were pretreated with either (A) a mitogen-activated protein kinase (ERK1/2) inhibitor (U1026 10 µM for 1 h), (B) a phosphatidylinositol 3-kinase (PI3K) inhibitor (LY 294002, 10 or 20 µM for 1 h) or an EGF receptor inhibitor (AG1478, 10 or 20 µM for 1 h) or (C) a protein kinase C general inhibitor (Bis 5 µM for 1 h) or the PKCδ specific inhibitor (rottlerin 5 µM for 1 h), before exposing them to asbestos (5 µg/cm<sup>2</sup>) for 24 h. RNA was prepared and analyzed by a ribonuclease protection assay. Quantitation of autoradiograms was performed using a phosphoimager. \**P* ≤ 0.05 as compared with respective untreated control, #*P* ≤ 0.05 as compared to respective asbestos-exposed group. All MMP12 studies were performed in fibroblasts whereas MMP13 and TIMP 1 studies were performed in lung epithelial type II cells (C10).

growth factor/PI3K/PKCδ/ERK1/2 dependent manner (Fig. 8). We also predict that MMPs activated by asbestos have the potential to further regulate asbestos-induced signaling pathways via activating EGFR in epithelial cells. The interplay between asbestos-induced MMPs and TIMPs may be crucial in the development of asbestos-induced lung diseases, and relevant signaling pathways may be targets for intervention and therapy. Though this study indicates that MMPs can regulate

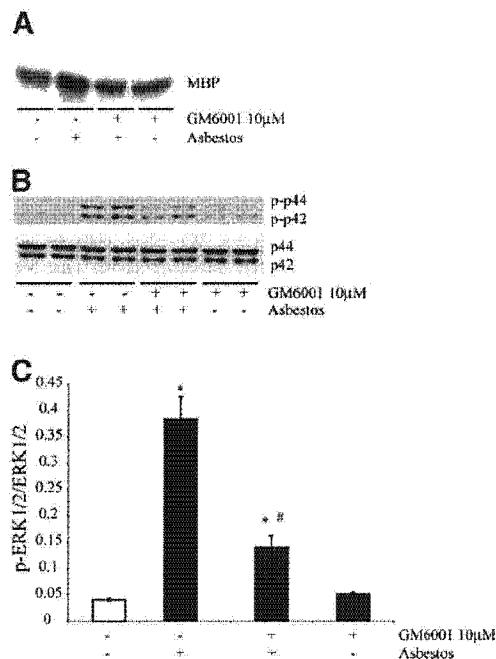


**Figure 7.** MMPs regulate asbestos-induced signaling pathways via EGFR activation in epithelial cells. Lung epithelial type II cells (C10) were pretreated with a broad-spectrum MMP inhibitor (GM6001, 10 µM) for 1 h before exposure with asbestos for 8 h. Western blot for ERK1/2 and EGFR kinase activity assays were performed as described in Materials and Methods. A) Kinase activity assay using MBP as a substrate showing inhibition of asbestos-induced EGFR activation by MMP inhibitor GM6001 (MBP = myelin basic protein). B) Western blot showing inhibition of asbestos-induced ERK1/2 (p-p44/p-p42) phosphorylation by GM6001. C) Quantitation of the Western blot in (B). \**P* ≤ 0.05 as compared to untreated control, #*P* ≤ 0.05 as compared with asbestos exposed group.

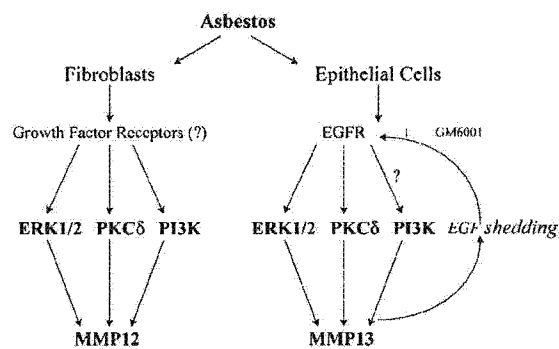


**Figure 8.** Hypothetical schema showing regulation of MMPs by asbestos. Asbestos exposure leads to up-regulation of MMPs via growth factor receptors, utilizing the ERK1/2, PKCδ, and PI3K pathways. Up-regulation and activation of MMPs may promote EGF shedding resulting in further EGFR activation and phosphorylation of ERK1/2 in epithelial cells. Inhibition of MMPs by the broad-spectrum inhibitor GM6001 prevents asbestos-induced EGFR activation and ERK1/2 phosphorylation in epithelial cells.